European Journal of Applied Mathematics (2025), 1–33
doi:10.1017/S0956792525100132

CAMBRIDGE UNIVERSITY PRESS

PAPER

A geometric approach to pinned pulses in a class of non-autonomous reaction–diffusion equations

Yuanxian Chen[1] and Jianhe Shen[1,2]

[1]College of Mathematics and Statistics, Fujian Normal University, Fuzhou, P.R. China
[2]Key Laboratory of Analytical Mathematics and Applications (Ministry of Education and Fujian Province) and Center for Applied Mathematics of Fujian Province, Fuzhou, P.R. China
Corresponding author: Jianhe Shen; Email: jhshen@fjnu.edu.cn

Received: 10 January 2025; **Revised:** 07 August 2025; **Accepted:** 09 August 2025

Keywords: non-autonomous reaction–diffusion equation; Gierer–Meinhardt equation; geometric singular perturbation theory; nonlocal eigenvalue problem

2020 Mathematics Subject Classification: 37B55, 35B35 (Primary); 35B25, 34D15 (Secondary)

Abstract

This paper develops a geometric and analytical framework for studying the existence and stability of pinned pulse solutions in a class of non-autonomous reaction–diffusion equations. The analysis relies on geometric singular perturbation theory, matched asymptotic method and nonlocal eigenvalue problem method. First, we derive the general criteria on the existence and spectral (in)stability of pinned pulses in slowly varying heterogeneous media. Then, as a specific example, we apply our theory to a heterogeneous Gierer–Meinhardt (GM) equation, where the nonlinearity varies slowly in space. We identify the conditions on parameters under which the pulse solutions are spectrally stable or unstable. It is found that when the heterogeneity vanishes, the results for the heterogeneous GM system reduce directly to the known results on the homogeneous GM system. This demonstrates the validity of our approach and highlights how the spatial heterogeneity gives rise to richer pulse dynamics compared to the homogeneous case.

1. Introduction

The spontaneous emergence of spatial patterns in reaction–diffusion (R–D) equations was first rigorously explained by Turing in his seminal work [34], where he demonstrated that diffusion-driven instability can destabilise homogeneous equilibria and give rise to non-trivial patterns when chemical species diffuse at disparate rates. Since then, R–D equations have become foundational in modelling diverse pattern formation in, for example, biology, chemistry and physics. The most interesting problem is the two-component R–D system with slow-fast diffusion described by

$$\begin{cases} \tau U_t = U_{xx} + H_1(U, U_x, V, V_x, \varepsilon), \\ V_t = \varepsilon^2 V_{xx} + H_2(U, U_x, V, V_x, \varepsilon), \end{cases} \tag{1.1}$$

where $\varepsilon > 0$ is sufficiently small; $x \in \mathbb{R}$ and $t \geq 0$ denote space and time, respectively; τ is the reaction time constant; and H_1 and H_2 are sufficiently smooth functions. Gray–Scott equation for autocatalytic reactions [6, 31, 33, 38] and Gierer–Meinhardt (GM) equation for morphogenesis [8, 19, 25, 40] are the typical examples. The existence and stability of localised patterns in these models, as well as other R–D systems [5, 10, 22, 29, 35], have been studied extensively. However, most previous studies focus on spatially homogeneous media. Though this assumption simplifies the underlying mathematical structure, it significantly limits the applicability of the models to realistic heterogeneous environments.

In contrast, heterogeneity is a ubiquitous phenomenon in nature, manifesting in diverse processes such as fluid convection in combustion, heterogeneous porous structures in solute transport, deposition processes and noise effects in biological systems. In recent decades, the impacts of spatial heterogeneity on the existence, stability and bifurcations of localised patterns in R–D equations have attracted significant attention; see, for example, [2, 3, 7, 15, 21, 36] and the references therein. Notably, heterogeneity breaks the translational invariance of the system, which makes the analysis more challenging.

In this paper, we investigate a singularly perturbed, non-autonomous two-component R–D system on the real line, namely,

$$\begin{cases} \varepsilon^2 U_t = U_{xx} - \varepsilon^2 \dfrac{\partial}{\partial U} W(U, \chi) - F(U, V), \\ V_t = \varepsilon^2 V_{xx} - G(U, V, \varepsilon), \end{cases} \tag{1.2}$$

where $U = U(x, t)$ and $V = V(x, t)$ denote the slow and fast components, respectively. The spatial heterogeneity is introduced through the potential $W(U, \chi)$, which is piecewise smooth in χ and exhibits a finite jump discontinuity at $\chi = \pm L$, where $\chi = \varepsilon x$ is a slow variable. This structure models an abrupt change in the underlying medium or energy landscape such as a sharp interface between distinct materials or biological domains. More precisely, we consider

$$W(U, \chi) = \begin{cases} W_1(U), & |\chi| > L, \\ W_2(U), & |\chi| < L \end{cases} \tag{1.3}$$

with $W_1(U) \not\equiv W_2(U)$; that is, the potentials $W(U, \chi)$ itself has a jump when $\chi = \pm L$. The resulting discontinuity in W breaks the translational invariance and induces spatial pinning of localised structures, a phenomenon that plays a central role in the emergence, stability and persistence of patterns in heterogeneous media.

The functions F, G, W_1 and W_2 are assumed to be sufficiently smooth. To proceed with our analysis, the following assumptions are needed:

- (A1) $G(U, 0, \varepsilon) = G_U(U, 0, \varepsilon) \equiv 0$, $G_V(U, 0, \varepsilon) > 0$ and $G_U(U, V, \varepsilon) > 0$ for $U, V > 0$.
- (A2) $F(U, 0) = F_U(U, 0) = F_V(U, 0) \equiv 0$.
- (A3) $W_1(U)$ has a local minimum at $U = 0$, that is, $\frac{\partial}{\partial U} W_1(0) = 0$ and $\frac{\partial^2}{\partial U^2} W_1(0) > 0$.
- (A4) For each $u > 0$, there exists a positive homoclinic solution $(v_0(\xi; u), q_0(\xi; u))$ to the following system:

$$\begin{cases} v' = q, \\ q' = G(u, v, 0), \end{cases}$$

such that $(v_0(\xi; u), q_0(\xi; u))$ converges to $(0, 0)$ as $|\xi| \to \infty$ and satisfies $q_0(0, u) = 0$. That is, for any $u > 0$, there exists $v_m > 0$ such that $\int_0^{v_m} G(u, s, 0)\, \mathrm{d}s = 0$.

Remark 1. If $W_1(U) = W_2(U)$, then $W(U, \chi) \equiv W_1(U)$, and system (1.2) reduces to the autonomous one

$$\begin{cases} \varepsilon^2 U_t = U_{xx} - \varepsilon^2 W_1'(U) - F(U, V), \\ V_t = \varepsilon^2 V_{xx} - G(U, V, \varepsilon). \end{cases} \tag{1.4}$$

- When $W_1'(U) = \alpha U$, $F(U, V) = -U^{a_1} V^{b_1}$ and $G(U, V, \varepsilon) = V - U^{a_2} V^{b_2}$, then system (1.4) is the generalised GM system, and in particular, it reduces to the classical GM equation when $a_1 = 0$, $a_2 = -1$ and $b_1 = b_2 = 2$.

https://doi.org/10.1017/S0956792525100132 Published online by Cambridge University Press

- When $W_1'(U) = \alpha(U-1)$, $F(U,V) = UV^2$ and $G(U,V,\varepsilon) = \beta V - UV^2$, then system (1.4) reduces to the Klausmeier–Gray–Scott system arising in many fields such as vegetative patterns [32] and phase transition [26].

The autonomous systems have translational invariance, while this property fails for the heterogeneous ones.

Doelman and Veerman [16] established the criteria for the existence and stability of pinned pulses in the general autonomous system (1.4). These criteria provide a theoretical framework for analysing pulse solutions in autonomous systems. However, the analysis becomes considerably complex for non-autonomous systems owing to the lack of translation invariance in non-autonomous equation (1.2). Thus, the methods developed in [12, 16, 37] for autonomous systems cannot be applied directly.

To address this issue, we extend the methodology developed in [11] to the non-autonomous equation (1.2). The approach developed in [11] is suitable for analysing pinned pulses in heterogeneous systems. In our current work, by integrating geometric singular perturbation theory (GSPT) [17] and the analytical frameworks established in [12] and [37], we investigate the formation of pinned pulses in non-autonomous system (1.2). Our analysis shows that equation (1.2) can admit multi-hump pinned pulse solutions. It is also found that the number of humps depends mainly on the spatial heterogeneity length $2L$ and the properties of the heterogeneous function $W(U,\chi)$. In contrast, for the autonomous case, the number of humps is at most two.

A central motivation for the present study is to investigate the GM system with jump-type spatial heterogeneities in its parameters. By introducing the discontinuities in the reaction and diffusion coefficients, the model captures a range of biologically and chemically relevant scenarios, in which the underlying medium exhibits abrupt spatial transitions. In fact, gene regulatory boundaries, cellular niche interfaces and spatially structured micro-environments are typical heterogeneities. Generally, the classical smooth models fail to reflect the discrete, compartmentalised organisation observed in real situations. In gene regulation, threshold-dependent activation of morphogen-responsive genes can lead to sharp on–off domains in gene expression, which is a behaviour that can be effectively modelled via spatially discontinuous reaction terms [24]. In developmental biology, niche transitions and tissue compartmentalisation such as those seen in limb formation or Drosophila wing patterning often give rise to abrupt changes in local kinetics and transport rates [4]. Likewise, heterogeneities in cellular microenvironments, including localised extracellular matrix structures or biochemical barriers, can create sharp spatial gradients in diffusion or reaction properties [27]. Wei and Winter [39] provided a rigorous analysis of the GM system with discontinuous diffusion coefficients, where it is shown that such jumps can induce spike pinning, asymmetry and even multistability.

The first main result of this article is the criteria for the existence of pinned pulse solutions to system (1.2). The existence of such pulses is governed by geometric conditions involving the phase space orbits of certain reduced Hamiltonian systems defined by the heterogeneous potential $W(U,\chi)$. Depending on the different signs of the points where the pinned pulse enters the heterogeneous region ($|\chi| < L$), denoted by (u_{in}, p_{in}), and the points where the pinned pulse enters the fast field ($|\xi| < 1/\sqrt{\varepsilon}$), denoted by (u_0, p_0), four distinct cases arise accordingly. Each case corresponds to a different class of orbit structures across the heterogeneous interface (see Figure 3).

Before we state the existence result, we need the following notations.

Notation 1. *We refer to the system*

$$\begin{cases} u_\chi = p, \\ p_\chi = W_i'(u), \end{cases} \qquad i = 1, 2 \tag{1.5}$$

the i-th system for convenience.

Notation 2. *Let* $\mathbf{P}$ *denote the set of closed orbits of the 2nd system restricted to the region* $u > 0$. *Given an energy level* $h \in \mathbf{P}$, *then the Hamiltonian*

https://doi.org/10.1017/S0956792525100132 Published online by Cambridge University Press

$$H_s(u,p) := \frac{1}{2}p^2 - W_2(u) = h$$

defines a periodic orbit. Otherwise, if $h \notin \mathbf{P}$*, then the corresponding trajectory is non-periodic. Moreover, let* $\mathbf{P}_1$ *denote the set of orbits of the 2nd system that possess a turning point (i.e.* $p = 0$*) in the region* $u > 0$*.*

Theorem 1. *Consider system (1.2) under the assumptions (A1)–(A4), and define*

$$\mathcal{H}(u_1,u_2,h) := \int_{u_2}^{u_1} \frac{du}{\sqrt{2h + 2W_2(u)}}.$$

If

$$\begin{cases} 0 = p_{in}^2 - 2W_1(u_{in}), \\ 2h = p_{in}^2 - 2W_2(u_{in}) \end{cases} \quad \text{and} \quad \begin{cases} p_0 = \mathcal{T}_-(u_0), \\ 2h = p_0^2 - 2W_2(u_0) \end{cases} \tag{1.6}$$

admit non-degenerate solutions $(u_{in}(h), p_{in}(h))$ *and* $(u_0(h), p_0(h))$*, respectively, with* $u_0 > u_{in}$*, then for sufficiently small* $\varepsilon > 0$*, the following statements hold:*

(i) If $p_0,\ p_{in} > 0$*, and there exists* $h_0 \notin \mathbf{P}$ *such that*

$$\mathcal{H}(u_0(h_0), u_{in}(h_0), h_0) = L, \tag{1.7}$$

or $h_0 \in \mathbf{P}$ *such that*

$$\mathcal{H}(u_0(h_0), u_{in}(h_0), h_0) = L \pmod{T}, \tag{1.8}$$

where

$$T = 2\int_{u_l(h_0)}^{u_r(h_0)} \frac{du}{\sqrt{2W_2(u) + 2h_0}},$$

in which $u_l(h_0)$ *and* $u_r(h_0)$ *are the intersection points of the periodic orbit with the u-axis, then system (1.2) admits pinned pulse solutions.*

(ii) If $p_0 < 0$ *and* $p_{in} > 0$*, and there exists* $h_0 \in \mathbf{P_1}$ *such that*

$$\mathcal{H}(u_0(h_0), u_{in}(h_0), h_0) + 2\mathcal{H}(u_t(h_0), u_0(h_0), h_0) = L, \tag{1.9}$$

where $(u_t(h_0), 0)$ *represents the turning point of the orbit of the 2nd system, and* $u_t(h_0) > u_0(h_0)$*, or there exists* $h_0 \in \mathbf{P}$ *such that*

$$\mathcal{H}(u_0(h_0), u_{in}(h_0)) + 2\mathcal{H}(u_r(h_0), u_0(h_0)) = L \pmod{T}, \tag{1.10}$$

then system (1.2) admits pinned pulse solutions.

(iii) If $p_0, p_{in} < 0$*, the 1st system has a homoclinic orbit connecting* $(0,0)$*, and there exists* $h_0 \in \mathbf{P}$ *such that*

$$2T - \mathcal{H}(u_0(h_0), u_{in}(h_0), h_0) = L \pmod{T}, \tag{1.11}$$

then system (1.2) admits pinned pulse solutions.

(iv) If $p_0 > 0$ *and* $p_{in} < 0$*, and the 1st system has a homoclinic orbit connecting* $(0,0)$*, and there exists* $h_0 \in \mathbf{P}$ *such that*

$$\mathcal{H}(u_{in}(h_0), u_l(h_0), h_0) + \mathcal{H}(u_0, u_l(h_0), h_0) = L \pmod{T}, \tag{1.12}$$

then system (1.2) admits pinned pulse solutions.

To determine the sufficient conditions for the (in)stability of pinned pulses, we analyse the point spectrum of the associated variational equation by using the Evans function. By the singularly perturbed structure of the underlying pulse solutions, the Evans function can be decomposed into the product of a fast transmission function and a slow transmission function. These transmission functions correspond to

https://doi.org/10.1017/S0956792525100132 Published online by Cambridge University Press

the lower-order eigenvalue problems that govern the leading order dynamics on the fast and slow scales. More precisely, the slow limiting eigenvalue problem is given by

$$(\text{slow}): \begin{cases} u_\chi = p, \\ p_\chi = \left(W''(u_{p,0}(\chi), \chi) + \lambda\right) u, \end{cases} \tag{1.13}$$

while the fast limiting eigenvalue problem takes the form

$$(\text{fast}): \begin{cases} v_\xi = q, \\ q_\xi = (G_v(u_0, v_0(\xi), 0) + \lambda)v + G_u(u_0, v_0(\xi), 0)\, \bar{u}(0). \end{cases} \tag{1.14}$$

Our analysis shows that the fast transmission function possesses a simple zero in the right half of the complex plane, that is, for values of λ with $\operatorname{Re}\lambda > 0$. However, the Evans function remains nonzero at this point due to the presence of a first-order pole in the slow transmission function. This implies that the '$\mathcal{O}(1)$-eigenvalues' generated by the fast transmission function are restricted to the stable left-half complex plane, that is, $\{\lambda \in \mathbb{C} \mid \operatorname{Re}\lambda < 0\}$.

In autonomous systems, due to the translational invariance, the eigenvalue $\lambda = 0$ remains a root of the fast transmission function for $0 < \varepsilon \ll 1$. However, for the non-autonomous system (1.2), this conclusion no longer holds. Consequently, the trivial eigenvalue may be perturbed to an '$\mathcal{O}(\varepsilon)$-eigenvalue', whose real part is either positive or negative. This subtle perturbation adds a new layer of complexity to the spectral stability problem. To overcome this difficulty, we derive sufficient conditions for instability by analysing the behaviour of the slow transmission function.

Let $(u_\pm(\chi, \lambda), p_\pm(\chi, \lambda))$ and $(v_\pm(\xi, \lambda), q_\pm(\xi, \lambda))$ denote solutions to the slow and fast limiting eigenvalue problems, respectively, which satisfy

$$\lim_{\chi \to \mp\infty} (u_\pm(\chi, \lambda), p_\pm(\chi, \lambda))\mathrm{e}^{\mp\Lambda_s(\lambda)\chi} = (1, \pm\Lambda_s(\lambda)),$$

$$\lim_{\xi \to \mp\infty} (v_\pm(\xi, \lambda), q_\pm(\xi, \lambda))\mathrm{e}^{\mp\Lambda_f(\lambda)\chi} = (1, \pm\Lambda_f(\lambda)),$$

where $\Lambda_f(\lambda) = \sqrt{G_v(0, 0, \varepsilon) + \lambda}$ and $\Lambda_s(\lambda) = \sqrt{W_1''(0) + \lambda}$.

Theorem 2. *The pinned pulses of system (1.2) are unstable if either of the following equations admits a root λ with positive real part:*

$$u_+(0, \lambda) = 0 \tag{1.15}$$

or

$$\mathcal{G}(\lambda) + 2\frac{p_+(0, \lambda)}{u_+(0, \lambda)} = 0, \tag{1.16}$$

where $u_+(0, \lambda) = u_+(\chi = 0, \lambda)$, $p_+(0, \lambda) = p_+(\chi = 0, \lambda)$, and

$$\mathcal{G}(\lambda) = \int_{-\infty}^{+\infty} \int_{-\infty}^{\xi} \left(F_u(u_0, v_0(\xi) + \frac{F_v(u_0, v_0(\xi))}{E_f(\lambda)} G_u(u_0, v_0(s), 0) v_+(s, \lambda) v_-(\xi, \lambda)\right) \mathrm{d}\, s\, \mathrm{d}\, \xi, \tag{1.17}$$

where $E_f(\lambda)$ is defined in (4.25).

The structure of this paper is as follows. In Section 2, we prove Theorem 1, which concerns the existence of stationary pinned pulse solutions for the general system (1.2) by GSPT and the technique of matching. Then in Section 3, we apply the results in Section 2 to a non-autonomous GM system to give the explicit existence of this explicit model. Based on the nonlocal eigenvalue problem (NLEP) method, Section 4 contains the analytical framework on the spectral stability for the general system (1.2) by computing the Evans function. These results are stated in Theorem 2. Finally, in Section 5, we apply the stability criteria in Section 4 to a non-autonomous GM system to identify the parameter under which the pinned pulses of this model are unstable.

https://doi.org/10.1017/S0956792525100132 Published online by Cambridge University Press

2. Proof of Theorem 1

A stationary pulse solution to (1.2) corresponds to a homoclinic orbit of the following 4-dimensional singularly perturbed ordinary differential system:

$$\begin{cases} \dot{u} = p, \\ \dot{p} = -\varepsilon^2 \dfrac{\partial}{\partial u} W(u, \chi) + F(u, v), \\ \varepsilon \dot{v} = q, \\ \varepsilon \dot{q} = G(u, v, \varepsilon), \end{cases} \tag{2.1}$$

where u and v represent the slow and fast variables, respectively, the dot indicates the differentiation in x and $0 < \varepsilon \ll 1$. To analyse the fast dynamics, we introduce a fast scale $\xi = \frac{x}{\varepsilon}$ to yield

$$\begin{cases} u' = \varepsilon p, \\ p' = \varepsilon^3 \dfrac{\partial}{\partial u} W(u, \chi) + \varepsilon F(u, v), \\ v' = q, \\ q' = G(u, v, \varepsilon), \end{cases} \tag{2.2}$$

where the prime denotes the differentiation in ξ. Systems (2.1) and (2.2) are equivalent if $\varepsilon \neq 0$.

Systems (2.1) and (2.2) are reversible with respect to

$$x, \xi \to -x, -\xi, \quad u \to u, \quad p \to -p, \quad v \to v, \quad q \to -q.$$

Due to the definition of $W(u, \chi)$ given in (1.3), $W(u, -\chi) = W(u, \chi)$ always holds. Together with the fact that $F(u, v)$ and $G(u, v, \varepsilon)$ do not explicitly depend on x, systems (2.1) and (2.2) remain invariant under the reversibility transformation mentioned above. This reversibility plays a crucial role in simplifying the forthcoming analysis on the existence and stability of pinned pulses.

2.1. Fast connections

Taking the singular limit $\varepsilon \to 0$ in (2.2) yields the limiting fast system

$$\begin{cases} v' = q, \\ q' = G(u, v, 0), \end{cases} \tag{2.3}$$

in which the slow variables (u, p) serve as parameters.

By the assumption (A1), $G(u, 0, 0) = 0$ holds for certain values of u. It thus follows that the set

$$\mathcal{M} = \{(u, p, v, q) | v = q = 0\}$$

consists of the equilibria of system (2.3). Furthermore, $\mathcal{M}$ is normally hyperbolic since $G_v(u, 0, \varepsilon) > 0$, which ensures that each equilibrium in $\mathcal{M}$ is a saddle of system (2.3). Consequently, both the stable and unstable manifolds $\mathcal{W}^s(\mathcal{M})$ and $\mathcal{W}^u(\mathcal{M})$ are 3-dimensional in the 4-dimensional phase space.

System (2.3) is integrable with the Hamiltonian

$$H(v, q; u) = \frac{1}{2} q^2 - \int_0^v G(u, s, 0)\, \mathrm{d}s. \tag{2.4}$$

The assumption (A4) ensures the existence of a homoclinic pulse in system (2.3). Moreover, the stable and unstable manifolds $\mathcal{W}^s(\mathcal{M})$ and $\mathcal{W}^u(\mathcal{M})$ coincide, forming a 3-dimensional homoclinic manifold, which is composed of a two-parameter family of homoclinic orbits (see Figure 1a).

When $\varepsilon > 0$ is sufficiently small, by GSPT, $\mathcal{M}$ perturbs to a 2-dimensional locally invariant manifold $\mathcal{M}_\varepsilon$, which is $\mathcal{O}(\varepsilon)$-close to its counterpart. Since $\mathcal{M}$ is invariant under the flow of $(2.2)_2$, it follows $\mathcal{M}_\varepsilon = \mathcal{M}$. Similarly, by GSPT again, $\mathcal{W}^{s/u}(\mathcal{M})$ perturbs to 3-dimensional locally invariant manifolds

https://doi.org/10.1017/S0956792525100132 Published online by Cambridge University Press

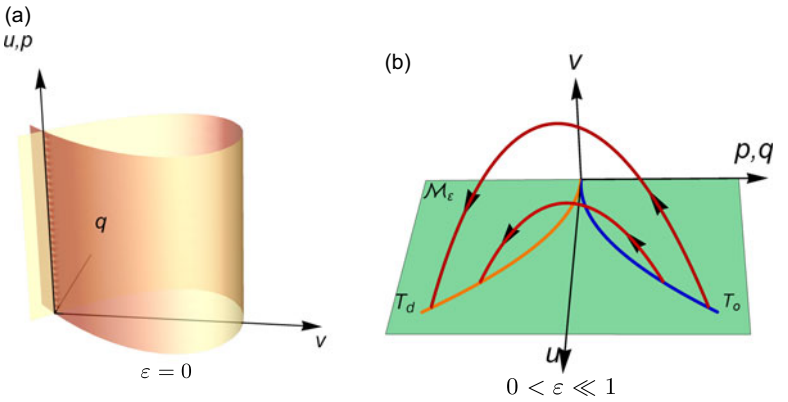

Figure 1. *(a) The 3-dimensional homoclinic manifold of the fast limiting system (2.3) at $\varepsilon = 0$. (b) A transversal intersection between $\mathcal{W}^s(\mathcal{M}_\varepsilon)$ and $\mathcal{W}^u(\mathcal{M}_\varepsilon)$ for $0 < \varepsilon \ll 1$, which is homoclinic to the slow manifold $\mathcal{M}_\varepsilon$.*

$\mathcal{W}^{s/u}(\mathcal{M}_\varepsilon)$, which are also $\mathcal{O}(\varepsilon)$-close to their counterparts. These manifolds consist of the fast stable and unstable fibres with their bases on the slow manifold $\mathcal{M}_\varepsilon$. When $0 < \varepsilon \ll 1$, $\mathcal{W}^s(\mathcal{M}_\varepsilon)$ and $\mathcal{W}^u(\mathcal{M}_\varepsilon)$ no longer coincide. Under appropriate conditions, they can intersect transversely, giving rise to a 2-dimensional manifold $\mathcal{W}^s(T_d) \cap \mathcal{W}^u(T_o)$ (see Remark 2 and Figure 1b).

Here, we want to remark that although the slow variables in system (2.2) are discontinuous due to the term $W(u, \chi)$, with each subregion, the system under consideration becomes autonomous with respect to χ. Thus, within each subregion, the standard framework of GSPT can still be applied to the two autonomous subsystems. At the positions of interfaces $\chi = \pm L$, we match the orbits of the two autonomous subsystems in a continuous, differentiable manner; that is, the orbits together with their derivatives are both connected. In this manner, we can still obtain the C^1-smooth orbits of the full system (2.2) by using GSPT within each smooth region and smooth matching at the position of heterogeneities.

We now employ the adiabatic Melnikov method [28, 30] to examine the persistence of the 3-dimensional homoclinic manifold, which is homoclinic to $\mathcal{M}_\varepsilon$ for $0 < \varepsilon \ll 1$. The analysis reveals that the homoclinic orbit acts as a dynamical bridge that enables the flow originating from the slow unstable manifold of the saddle on $\mathcal{M}_\varepsilon$ to return to the slow stable manifold, thereby facilitating a dynamical transition.

To facilitate the analysis, we partition the entire spatial interval $(-\infty, +\infty)$ into three subregions, namely, two slow regions $I_s^- = (-\infty, -\frac{1}{\sqrt{\varepsilon}})$ and $I_s^+ = (\frac{1}{\sqrt{\varepsilon}}, \infty)$ and a fast region $I_f = [-\frac{1}{\sqrt{\varepsilon}}, \frac{1}{\sqrt{\varepsilon}}]$. The boundaries of the fast region I_f are placed in the transition zone, satisfying $|\xi| \gg 1$ and $|x| \ll 1$. In other words, the exact location of ∂I_f is not critical [12, 16]. Indeed, the width of I_f should be chosen appropriately to ensure that $v_h(\xi)$ is exponentially small everywhere outside I_f, while $u_h(\xi)$ remains approximately constant, to the leading order, within the fast region I_f.

Remark 2. For convenience, we denote by $\mathcal{W}^u(T_o)$ the collection of unstable fibres with base points on the curve T_o and by $\mathcal{W}^s(T_d)$ the collection of stable fibres with base points on the curve T_d. These sets intersect forming a 2-dimensional manifold, denoted as $\mathcal{W}^s(T_d) \cap \mathcal{W}^u(T_o)$. In the subsequent analysis, we will prove that

$$\mathcal{W}^s(\mathcal{M}_\varepsilon) \cap \mathcal{W}^u(\mathcal{M}_\varepsilon) = \mathcal{W}^s(T_d) \cap \mathcal{W}^u(T_o). \tag{2.5}$$

Remark 3. In our setup, the heterogeneity region $[-L, L]$ is defined in terms of the super-slow spatial variable $\chi = \varepsilon x = \varepsilon^2 \xi$, as introduced in equation (1.2). Thus, in terms of the original spatial variable ξ, the corresponding heterogeneous region is rescaled to $\left[-\frac{L}{\varepsilon^2}, \frac{L}{\varepsilon^2}\right]$, which becomes much wider as $\varepsilon \to 0$.

https://doi.org/10.1017/S0956792525100132 Published online by Cambridge University Press

On the other hand, the fast region is defined as $I_f = \left[-\frac{1}{\sqrt{\varepsilon}}, \frac{1}{\sqrt{\varepsilon}}\right]$. Therefore, we have

$$\left[-\frac{1}{\sqrt{\varepsilon}}, \frac{1}{\sqrt{\varepsilon}}\right] \subset \left[-\frac{L}{\varepsilon^2}, \frac{L}{\varepsilon^2}\right].$$

In the fast system (2.2), the Hamiltonian $H(v, q; u)$ becomes a slowly varying function. Its derivative with respect to the fast time variable ξ is given by

$$H_\xi(v, q; u) = \big(G(u, v, \varepsilon) - G(u, v, 0)\big)q - \varepsilon p \int_0^v G_u(u, s, 0)\, \mathrm{d}s + \mathcal{O}(\varepsilon^2). \tag{2.6}$$

The unperturbed homoclinic orbit $(u^{(0)}, p^{(0)}, v_0(\xi), q_0(\xi))$ is perturbed to a solution of the full fast system (2.2), denoted by

$$\gamma_h(\xi) = (u_h(\xi),\ p_h(\xi),\ v_h(\xi),\ q_h(\xi))\,,$$

which is homoclinic to $\mathcal{M}_\varepsilon$, provided that the Melnikov integral

$$\begin{aligned} \triangle_{I_f} H(u, p) = &\int_{I_f} \big(G(u_h(\xi), v_h(\xi), \varepsilon) - G(u_h(\xi), v_h(\xi), 0)\big) q_h(\xi)\, \mathrm{d}\xi \\ &- \varepsilon \int_{I_f} p_h(\xi) \int_0^{v_h(\xi)} G_u(u_h(\xi), s, 0)\, \mathrm{d}s\mathrm{d}\xi + \mathcal{O}(\varepsilon^2) \end{aligned} \tag{2.7}$$

has a simple zero. In that case, we have $\gamma_h(\xi) \subset \mathcal{W}^s(\mathcal{M}_\varepsilon) \cap \mathcal{W}^u(\mathcal{M}_\varepsilon)$. The improper integral is well-defined because $\gamma_h(\xi)$ converges exponentially to $(0, 0, 0, 0)$ as $\xi \to \pm\infty$.

To leading order,

$$\begin{aligned} \triangle_{I_f} H(u^{(0)}, p^{(0)}) = &\int_{I_f} \big(G(u^{(0)}, v_0(\xi), \varepsilon) - G(u^{(0)}, v_0(\xi), 0)\big) q_0(\xi)\, \mathrm{d}\xi \\ &- \varepsilon \int_{I_f} p^{(0)} \int_0^{v_0(\xi)} G_u(u^{(0)}, s, 0)\, \mathrm{d}s\mathrm{d}\xi. \end{aligned} \tag{2.8}$$

Since $v_0(\xi)$ is even and $q_0(\xi)$ is odd, so $\big(G(u^{(0)}, v_0(\xi), \varepsilon) - G(u^{(0)}, v_0(\xi), 0)\big)$ and $\int_0^{v_0(\xi)} G_u(u^{(0)}, s, 0)\ \mathrm{d}s$ are even functions. Note that $u^{(0)}$ is assumed to be positive; it then follows from (A1) that $G_u(u^{(0)}, v, 0)$ is also positive. Consequently, solving $\triangle_{I_f} H(u^{(0)}, p^{(0)}) = 0$ gives $p^{(0)} = 0$.

To compute the correction, we expand $(u_h(\xi), p_h(\xi), v_h(\xi), q_h(\xi))$ in the power of ε, namely,

$$\begin{aligned} u_h(\xi) &= u^{(0)} + \varepsilon u_1(\xi) + \text{h.o.t.}, \\ p_h(\xi) &= \varepsilon p_1(\xi) + \text{h.o.t.}, \\ v_h(\xi) &= v_0(\xi) + \text{h.o.t.}, \\ q_h(\xi) &= q_0(\xi) + \text{h.o.t.}, \end{aligned} \tag{2.9}$$

where the initial conditions are $u_h(0) = u^{(0)}$ and $u_j(0) = 0$ for all $j \geq 1$. Substituting (2.9) into (2.2) gives

$$u_1(\xi) \equiv 0, \quad p_1(\xi) = \int_0^\xi F\big(u^{(0)}, v_0(\omega)\big)\, \mathrm{d}\omega + p_1(0).$$

https://doi.org/10.1017/S0956792525100132 Published online by Cambridge University Press

Note that the integral term in $p_1(\xi)$ is an odd function since $v_0(\xi)$ is an even function; thus, (2.7) becomes

$$\begin{aligned}\int_{I_f} H_\xi \,\mathrm{d}\xi &= \int_{-\infty}^{+\infty} \big(G(u^{(0)}, v_0(\xi), \varepsilon) - G(u^{(0)}, v_0(\xi), 0)\big) q_0(\xi)\,\mathrm{d}\xi \\ &\quad - \varepsilon \int_{-\infty}^{+\infty} (p^{(0)} + \varepsilon p_1(\xi)) \int_0^{v_0(\xi)} G_u(u^{(0)}, s, 0)\ \mathrm{d}s\mathrm{d}\xi + \text{h.o.t.} \\ &= -2\varepsilon(p^{(0)} + \varepsilon p_1(0)) \int_0^{+\infty} \int_0^{v_0(\xi)} G_u(u^{(0)}, s, 0)\,\mathrm{d}s\,\mathrm{d}\xi + \text{h.o.t.}\end{aligned} \tag{2.10}$$

Since u_0 is positive, the integral in (2.10) is also positive by the assumption (A1). Therefore, we conclude that the condition for vanishing Melnikov integral up to $\mathcal{O}(\varepsilon^2)$ is

$$p^{(0)} = 0, \qquad p_1(0) = 0.$$

Remark 4. For any orbit

$$\gamma_h(\xi) = (u_h(\xi), p_h(\xi), v_h(\xi), q_h(\xi)) \subset \mathcal{W}^s(\mathcal{M}_\varepsilon) \cap \mathcal{W}^u(\mathcal{M}_\varepsilon),$$

it follows from the reversibility symmetry that

$$u_h(\xi) = u_h(-\xi), \qquad v_h(\xi) = v_h(-\xi). \tag{2.11}$$

Therefore, $\xi = 0$ must be an extremum (specifically, a local maximum) of both $u_h(\xi)$ and $v_h(\xi)$. By Fermat's Lemma, this yields $p_h(0) = 0$ and $q_h(0) = 0$.

Define the Take-off curve T_o and the Touch-down curve T_d on $\mathcal{M}_\varepsilon$ by

$$T_{o/d} = \left\{ (u, p, v, q) \,\middle|\, u = u_h\left(\mp\frac{1}{\sqrt{\varepsilon}}\right),\ p = p_h\left(\mp\frac{1}{\sqrt{\varepsilon}}\right),\ v = q = 0 \right\} \tag{2.12}$$

with $p = \frac{1}{\varepsilon}\frac{du}{d\xi}$. By (2.2), we have

$$\begin{aligned}\Delta u &= \int_{I_f} u_\xi \,\mathrm{d}\xi = \int_{I_f} \varepsilon^2 p_1(\xi)\,\mathrm{d}\xi = \mathcal{O}(\varepsilon^{3/2}), \\ \Delta p &= \int_{I_f} p_\xi \,\mathrm{d}\xi = \int_{I_f} \varepsilon F(u, v(\xi)) + \mathcal{O}(\varepsilon^3)\,\mathrm{d}\xi \\ &= 2\varepsilon \int_{-\infty}^{0} F(u, v_0(\xi))\ \mathrm{d}\xi + \mathcal{O}(\varepsilon^2),\end{aligned} \tag{2.13}$$

where we have used the facts that $u_\xi = \varepsilon p$ and $p = \mathcal{O}(\varepsilon)$ during I_f in the first equation, and $v_0(\xi)$ is an even function with respect to ξ in the second equation. So, to leading order, the explicit representations of the Take-off curve T_o and the Touch-down curve T_d on $\mathcal{M}_\varepsilon$ are, respectively

$$T_{o,d}(u) = \big\{ (u, p, 0, 0) \in \mathcal{M}_\varepsilon \mid p = \mathcal{T}_\mp(u) + \mathcal{O}(\varepsilon^2),\ u > 0 \big\}, \tag{2.14}$$

where $\mathcal{T}_\mp(u) = \mp\varepsilon \int_{-\infty}^{0} F(u, v_0(\xi))\,\mathrm{d}\xi$ and $p = \frac{1}{\varepsilon}\frac{du}{d\xi}$.

Remark 5. The homoclinic solution $(v_0(\xi; u), q_0(\xi; u))$ of system (2.3) provides the leading order solution of (2.2), given by

$$\phi_h(\xi) := \left(u, \varepsilon \int_0^\xi F(u, v_0(x; u))\,\mathrm{d}x, v_0(\xi; u), q_0(\xi; u) \right), \tag{2.15}$$

which is homoclinic to $\mathcal{M}_\varepsilon$. Moreover, its asymptotic limits $\lim_{\xi\to\pm\infty} \phi_h(\xi)$ correspond precisely to the Touch-down and Take-off curves.

https://doi.org/10.1017/S0956792525100132 Published online by Cambridge University Press

2.2. Slow dynamics on the slow manifold

A singular homoclinic orbit is constructed by concatenating trajectories of the fast and slow limiting systems. Though this singular homoclinic orbit is not an exact solution to system (2.2), GSPT ensures that a true homoclinic orbit exists within a small neighbourhood of this singular trajectory. In the previous subsection, the trajectories of the fast limiting system had been derived. In this section, we focus on the slow dynamics on the slow manifold and match them with the fast segments to complete the full orbit.

On the slow manifold

$$\mathcal{M}_\varepsilon = \{(u, p, v, q) | v = q = 0,\ u > 0\}, \tag{2.16}$$

the dynamics of system (2.2) are governed by

$$u_{\xi\xi} = \varepsilon^4 \frac{\partial}{\partial u} W(u, \chi). \tag{2.17}$$

In the super-slow coordinate $\chi = \varepsilon^2 \xi$, the slow limiting system can be transformed into

$$\begin{cases} u_\chi = p, \\ p_\chi = \dfrac{\partial}{\partial u} W(u, \chi), \end{cases} \tag{2.18}$$

which is a non-autonomous Hamiltonian system with

$$H_s(u, p) = \frac{1}{2} p^2 - W(u, \chi). \tag{2.19}$$

It follows from (A3) that system (2.18) admits a saddle $(0, 0)$. The slow trajectories can be constructed via the phase plane analysis on two autonomous Hamiltonian systems,

$$\begin{cases} u_\chi = p, \\ p_\chi = W_i'(u), \end{cases} \qquad i = 1, 2, \tag{2.20}$$

where $W_i'(u)$ are the potentials outside and inside the heterogeneous region, respectively. Appropriate boundary conditions must be imposed to ensure that the matching between the trajectories and their derivatives at the endpoints of each region can be performed. These trajectories decay exponentially to $(0, 0)$ as $\chi \to \pm\infty$. In this manner, the solutions to system (2.18) are C^1-smooth.

In the following, we will demonstrate that the value of the Hamiltonian h inside the heterogeneity with the length $2L$ serves as an important parameter to characterise the pinned pulses. A pinned pulse is generally determined by four points in the phase plane, namely:

- The points where the pinned pulse enters and exits the heterogeneous region, respectively, denoted by (u_{in}, p_{in}) and (u_{out}, p_{out}).
- The points where the pinned pulse enters and exits the fast field, respectively, denoted by (u_0, p_0) and (u_d, p_d).

Since system (2.2) is symmetric under $\chi \to -\chi$, we have

$$u_{in} = u_{out}, \qquad p_{in} = -p_{out},$$
$$u_0 = u_d, \qquad p_0 = -p_d.$$

Therefore, only (u_{in}, p_{in}) and (u_0, p_0) need to be determined. More precisely, (u_{in}, p_{in}) is the intersection between the unstable manifold of the saddle $(0, 0)$ outside the heterogeneity (the purple solid curve in Figure 2) and the level set $H_s(u, p) = h$ within the heterogeneous region (the black curve). They satisfy

$$\begin{aligned} 0 &= p_{in}^2 - 2W_1(u_{in}), \\ 2h &= p_{in}^2 - 2W_2(u_{in}), \end{aligned} \tag{2.21}$$

https://doi.org/10.1017/S0956792525100132 Published online by Cambridge University Press

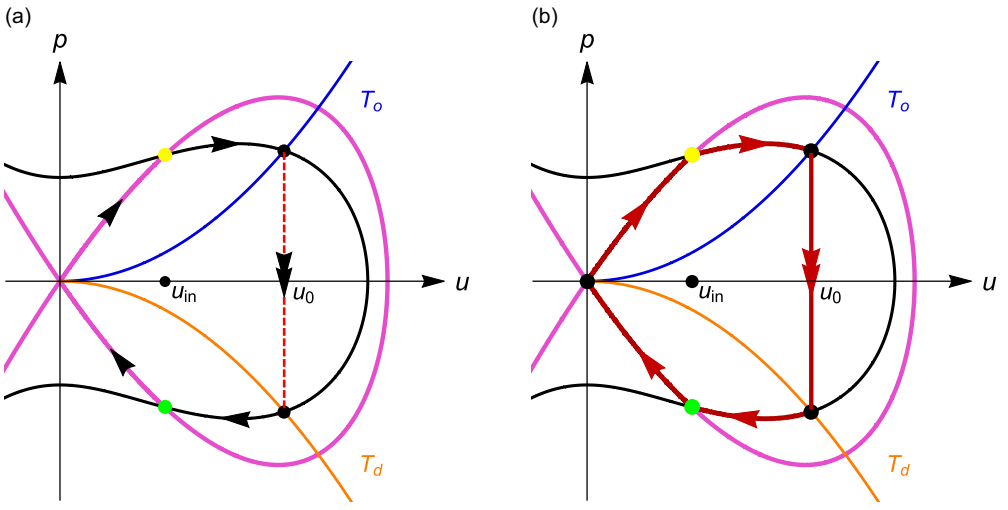

Figure 2. *Singular homoclinic orbit of system (2.2) with* 1 *fast and* 4 *slow segments. Left panel: two slow segments outside the heterogeneity are marked by the solid purple curves, indicating the stable and unstable manifolds of the saddle* $(0, 0)$*; two slow segments inside the heterogeneity (the black curves), representing the orbits defined by* $H_s(u, p) = h$*; and a fast segment is indicated by the red dashing line. In the figure, the yellow dot represents* (u_{in}, p_{in})*, and the green one stands for* (u_{out}, p_{out})*. Right panel: the thick red curve indicates the whole singular homoclinic orbit.*

where

$$W_1'(u_{in}) - W_2'(u_{in}) \neq 0$$

is required to ensure that the intersection between such two slow trajectories is transverse, and h represents the Hamiltonian value within the heterogeneity. By solving system (2.21), we can obtain $(u_{in}, p_{in}) = (u_{in}(h), p_{in}(h))$, where h acts as a free parameter.

Remark 6. Let $u = u_{in,k} > 0$, $k = 1, 2, \cdots, K$, be the K non-degenerate solutions obtained from (2.21), then there exist $2K$ distinct points $(u_{in,k}, p^{\pm}_{in,k})$. These points play a key role in constructing the transversely intersecting homoclinic orbits.

Based on the curves $T_{o,d}$ on $\mathcal{M}_\varepsilon$ defined in (2.14), a homoclinic orbit ϕ_h of the limiting fast system (2.3) can be connected with the slow orbits on the slow manifold $\mathcal{M}_\varepsilon$ to construct a singular homoclinic orbit. To guarantee that this singular orbit persists under small perturbations, it is essential that the Take-off curve T_o intersects transversely with the orbit of the 2nd system (2.20). The corresponding intersection point (u_0, p_0) is governed by

$$\begin{aligned} p_0 &= \mathcal{T}_-(u_0), \\ 2h &= p_0^2 - 2W_2(u_0), \end{aligned} \tag{2.22}$$

where it is also required that

$$\mathcal{T}_-(u_0)\mathcal{T}_-'(u_0) - W_2'(u_0) \neq 0$$

such that the matching is transverse.

If both equations (2.21) and (2.22) admit non-degenerate solutions $(u_{in}(h), p_{in}(h))$ and $(u_0(h), p_0(h))$, this implies that

- The outer and inner slow trajectories intersect transversely at the position of heterogeneity.
- The slow trajectory intersects with the fast jump trajectory transversely.

https://doi.org/10.1017/S0956792525100132 Published online by Cambridge University Press

However, the Hamiltonian value h remains undetermined now. To determine it, we impose the condition that the 'time' for the slow trajectory to evolve from $(u_{in}(h), p_{in}(h))$ to $(u_0(h), p_0(h))$ is exactly L (the half-width of the heterogeneous region). Once this condition is satisfied, we get a singular homoclinic orbit from the saddle to itself with transversality. By GSPT, there are true homoclinic orbits in a small neighbourhood of this singular configuration.

Remark 7. The relative positions of (u_{in}, p_{in}) and (u_0, p_0), respectively, determined by (2.21) and (2.22) are crucial for constructing the different types of singular homoclinic orbits. It is worth noting that the orbits in the 2nd system possessing through 'turning points' are particularly important for constructing pinned pulses with certain dynamical properties.

Remark 8. Theorem 1 gives the case $u_0 > u_{in}$. Similar results can be obtained when $u_0 < u_{in}$, where system (1.2) can also admit pinned pulse solutions.

3. Pinned pulses in a non-autonomous Gierer–Meinhardt equation

Consider

$$\begin{cases} \varepsilon^2 U_t = \quad U_{xx} - \varepsilon^2 (f(\chi)U - g(\chi)U^d) + \sigma V^2, \\ V_t = \varepsilon^2 V_{xx} - V + \dfrac{V^2}{U}, \end{cases} \tag{3.1}$$

where $\sigma \neq 0$, $d > 1$ and

$$f(\chi) = \begin{cases} \alpha_1, & |\chi| > L, \\ \alpha_2, & |\chi| < L, \end{cases} \qquad g(\chi) = \begin{cases} \gamma_1, & |\chi| > L, \\ \gamma_2, & |\chi| < L. \end{cases} \tag{3.2}$$

The associated fast limiting system is

$$\begin{cases} v' = q, \\ q' = v - \dfrac{v^2}{u}, \end{cases} \tag{3.3}$$

which admits a saddle $(0, 0)$ and a homoclinic orbit described by

$$\begin{aligned} v_0(\xi, u) &= \frac{3u}{2} \operatorname{sech}^2\left(\frac{\xi}{2}\right), \\ q_0(\xi, u) &= -\frac{3u}{2} \operatorname{sech}^2\left(\frac{\xi}{2}\right) \tanh\left(\frac{\xi}{2}\right). \end{aligned} \tag{3.4}$$

The explicit homoclinic orbit solution (3.4) of (3.3) is well-known (see, e.g. [31, 37]). By direct calculations, the Take-off and Touch-down curves are, respectively

$$T_{o/d}(u) = \left\{ (u, p, 0, 0) \in \mathcal{M}_\varepsilon \mid p = \pm 3\varepsilon\sigma u^2 + \mathcal{O}(\varepsilon^2),\ u > 0 \right\}. \tag{3.5}$$

Note that for $\sigma > 0$, the Take-off curve lies in the first quadrant of the (u, p) plane, while for $\sigma < 0$, it lies in the fourth quadrant. Thus, changing the sign of σ reverses the direction of the fast jump (see Figures 3 and 4).

The limiting slow system corresponding to (2.18) becomes

$$\begin{cases} u_\chi = p, \\ p_\chi = f(\chi)u - g(\chi)u^d, \end{cases} \tag{3.6}$$

https://doi.org/10.1017/S0956792525100132 Published online by Cambridge University Press

which has a saddle at $(0,0)$ when $\alpha_1 > 0$. This is a piecewise Hamiltonian system with

$$H_s(u,p) = \frac{1}{2}p^2 - \left(\frac{f(\chi)}{2}u^2 - \frac{g(\chi)}{d+1}u^{d+1}\right). \tag{3.7}$$

The matching condition for the entry point (u_{in}, p_{in}) is given by

$$\begin{aligned} 0 &= p_{in}^2 - \left(\alpha_1 u_{in}^2 - \frac{2\gamma_1}{d+1}u_{in}^{d+1}\right), \\ 2h &= p_{in}^2 - \left(\alpha_2 u_{in}^2 - \frac{2\gamma_2}{d+1}u_{in}^{d+1}\right), \\ 0 &\neq (\alpha_1 - \alpha_2)u_{in} - (\gamma_1 - \gamma_2)u_{in}^d, \end{aligned} \tag{3.8}$$

where h represents the Hamiltonian within the heterogeneous region. Similarly, the matching condition between the slow and fast orbits can be given by

$$\begin{aligned} p_0 &= 3\sigma u_0^2, \\ 2h &= p_0^2 - \left(\alpha_2 u_0^2 - \frac{2\gamma_2}{d+1}u_0^{d+1}\right), \\ 0 &\neq 18\sigma^2 u_0^3 - \left(\alpha_2 u_0 - \gamma_2 u_0^d\right). \end{aligned} \tag{3.9}$$

In what follows, we consider two distinct cases.

3.1. *Case 1:* $g(\chi) \equiv 0$.

Through this simplest case, we can illustrate the key idea of the geometric approach clearly.

Under $g(\chi) \equiv 0$, the matching conditions in equation (3.8) reduce to

$$\begin{aligned} 0 &= p_{in}^2 - \alpha_1 u_{in}^2, \\ 2h &= p_{in}^2 - \alpha_2 u_{in}^2. \end{aligned} \tag{3.10}$$

Solving these two equations yields the explicit expressions for u_{in} and p_{in} in terms of h, namely,

$$u_{in}(h) = \sqrt{\frac{2h}{\alpha_1 - \alpha_2}}, \qquad p_{in}(h) = \sqrt{\frac{2h\alpha_1}{\alpha_1 - \alpha_2}}, \tag{3.11}$$

where $\text{sign}(h) = \text{sign}(\alpha_1 - \alpha_2)$, which ensures that $u_{in}(h),\ p_{in}(h) > 0$. By direct calculations, when $\sigma > 0$ and $\text{sign}(h) = \text{sign}(\alpha_1 - \alpha_2)$, (3.9) can be simplified as

$$u_0(h) = u_0^{\pm}(h) = \frac{\left(\alpha_2 \pm \sqrt{\alpha_2^2 + 72\sigma^2 h}\right)^{\frac{1}{2}}}{3\sqrt{2}\sigma}, \tag{3.12}$$

where we only consider $u_0(h) \in \mathbb{R}_+$ ($u_0(h) = u_0^-(h)$ is valid only when $\alpha_1 < \alpha_2$, which is discarded). Thus, the condition $u_0(h) > u_{in}(h)$ is equivalent to

$$\frac{\left(\alpha_2 \pm \sqrt{\alpha_2^2 - 72\sigma^2 h}\right)^{\frac{1}{2}}}{3\sqrt{2}\sigma} > \sqrt{\frac{2h}{\alpha_1 - \alpha_2}}. \tag{3.13}$$

Within the heterogeneous region, the slow orbit satisfies

$$2h = p^2 - \alpha_2 u^2$$

https://doi.org/10.1017/S0956792525100132 Published online by Cambridge University Press

with $p = u_\chi$. Therefore, the relationship between the length L and the Hamiltonian h is

$$L = \int_{-L}^{0} \mathrm{d}x = \int_{u_{in}(h)}^{u_0(h)} \frac{\mathrm{d}u}{p} = \int_{u_{in}(h)}^{u_0(h)} \frac{\mathrm{d}u}{\sqrt{2h + \alpha_2 u^2}} = I(u_0(h)) - I(u_{in}(h)), \tag{3.14}$$

where

$$I(u) = \begin{cases} \dfrac{1}{\sqrt{\alpha_2}} \log\ (2\sqrt{\alpha_2(2h + \alpha_2 u^2)} + 2\alpha_2 u), & [\alpha_2 u > \sqrt{-\Delta}, \quad \Delta < 0], \\ \dfrac{1}{\sqrt{\alpha_2}} \log\ (\sqrt{\alpha_2(2h + \alpha_2 u^2)} - 2\alpha_2 u), & [2\alpha_2 u < -\sqrt{-\Delta}, \quad \Delta < 0], \\ \dfrac{1}{\sqrt{\alpha_2}} \operatorname{arcsinh}\left(\dfrac{\alpha_2 u}{\sqrt{\Delta}}\right), & [\Delta > 0], \\ \dfrac{1}{\sqrt{\alpha_2}} \log\ (2\alpha_2 u), & [\Delta = 0], \end{cases} \tag{3.15}$$

and $\Delta = \alpha_2 h$. By combining (3.11), (3.12) and (3.14), the value of h can be implicitly determined. This determines the exact slow orbit used in the construction of the pinned pulse solution.

The unstable and stable manifolds of the saddle $(0, 0)$ are given by

$$u_{h,\mp}(\chi) = e^{\pm\sqrt{\alpha_1}(\chi \mp x_*)}, \tag{3.16}$$

where $x_* > 0$ is introduced such that $u_{h,-}(-L) = u_{in}$. By the reversible symmetry, it follows that $u_{h,+}(L) = u_{out}$. Within the heterogeneous region ($|x| < L$), the expression of the orbit is given explicitly by

$$u_{i,\mp}(\chi) = A_{1,2} e^{-\sqrt{\alpha_2}\chi} + B_{1,2} e^{\sqrt{\alpha_2}\chi}, \tag{3.17}$$

where the constants $A_{1,2}$ and $B_{1,2}$ are determined to ensure that $u_{p,0}(\chi)$ is continuously differentiable at $\chi = \pm L$. Thus, the composite solution can be defined by

$$u_{p,0}(\chi) = \begin{cases} u_{h,-}(\chi), & \chi \in (-\infty, -L), \\ u_{i,-}(\chi), & \chi \in (-L, 0), \\ u_{i,+}(\chi), & \chi \in (0, L), \\ u_{h,+}(\chi), & \chi \in (L, +\infty). \end{cases} \tag{3.18}$$

Hence, the smooth matching condition at $\chi = \pm L$ is given by

$$\begin{pmatrix} e^{\sqrt{\alpha_2}L} & e^{-\sqrt{\alpha_2}L} & 0 & 0 \\ -\sqrt{\alpha_2} e^{\sqrt{\alpha_2}L} & \sqrt{\alpha_2} e^{-\sqrt{\alpha_2}L} & 0 & 0 \\ 0 & 0 & e^{-\sqrt{\alpha_2}L} & e^{\sqrt{\alpha_2}L} \\ 0 & 0 & -\sqrt{\alpha_2} e^{-\sqrt{\alpha_2}L} & \sqrt{\alpha_2} e^{\sqrt{\alpha_2}L} \end{pmatrix} \begin{pmatrix} A_1 \\ B_1 \\ A_2 \\ B_2 \end{pmatrix} = \begin{pmatrix} u_{in} \\ p_{in} \\ u_{out} \\ p_{out} \end{pmatrix}. \tag{3.19}$$

Solving (3.19) directly yields

$$\begin{aligned} A_1 = B_2 &= \frac{(\sqrt{\alpha_2}\, u_{in} - p_{in}) e^{-\sqrt{\alpha_2}L}}{2\sqrt{\alpha_2}} = \frac{\alpha_2 - \sqrt{\alpha_1 \alpha_2}}{2\alpha_2} \sqrt{\frac{2h}{\alpha_1 - \alpha_2}}\, e^{-\sqrt{\alpha_2}L}, \\ B_1 = A_2 &= \frac{(\sqrt{\alpha_2} u_{in} + p_{in}) e^{\sqrt{\alpha_2}L}}{2\sqrt{\alpha_2}} = \frac{\alpha_2 + \sqrt{\alpha_1 \alpha_2}}{2\alpha_2} \sqrt{\frac{2h}{\alpha_1 - \alpha_2}}\, e^{\sqrt{\alpha_2}L}. \end{aligned} \tag{3.20}$$

Theorem 3. *Let $\varepsilon > 0$ be sufficiently small, and α_1, α_2, σ, $L > 0$ be given. Assume that (3.13) admits a non-degenerate root h satisfying $\mathrm{sign}(h) = \mathrm{sign}(\alpha_1 - \alpha_2)$ and that (3.14) holds, then system (3.1) with $g(\chi) \equiv 0$ admits a pinned pulse solution $(u_h(\xi), v_h(\xi))$ with*

$$|v_h(\xi) - v_0(\xi; u_0(h_0))|, \ \ |u_h(\xi) - u_0(h_0)| = \mathcal{O}(\varepsilon), \tag{3.21}$$

https://doi.org/10.1017/S0956792525100132 Published online by Cambridge University Press

for $\xi \in I_f$, where $v_0(\xi; u_0(h))$ and $u_0(h)$ are given by (3.4) and (3.12), respectively. For $\xi \in I_s^{\pm}$, we have

$$|v_h(\xi)|, \ \ |u_h(\chi) - u_{p,0}(\chi)| = \mathcal{O}(\varepsilon), \tag{3.22}$$

where $u_{p,0}(\chi)$ is defined in (3.18).

3.2. *Case 2:* $g(\chi) \neq 0$.

In the previous subsection, we study the $g(\chi) \equiv 0$ case; that is, the slow limiting system is piecewise linear. When $g(\chi) \neq 0$, the system becomes piecewise nonlinear, leading to significantly increased complexity.

Outside the heterogeneous region ($|\chi| > L$), equation (3.6) turns out to be

$$u_{\chi\chi} = \alpha_1 u - \gamma_1 u^d. \tag{3.23}$$

When $\alpha_1, \gamma_1 > 0$, this equation admits a homoclinic orbit given by

$$u_{h,0}(\chi) = \left[\frac{\alpha_1(d+1)}{2\gamma_1}\operatorname{sech}^2\left(\frac{d-1}{2}\sqrt{\alpha_1}\chi\right)\right]^{\frac{1}{d-1}}. \tag{3.24}$$

Therefore, the unstable and stable manifolds of the saddle $(0,0)$ outside the heterogeneous region can be, respectively, parameterised by

$$\begin{aligned} u_{h,-}(\chi) &= \left[\frac{\alpha_1(d+1)}{2\gamma_1}\operatorname{sech}^2\left(\frac{d-1}{2}\sqrt{\alpha_1}(\chi - \operatorname{sign}(p_{in})x_*)\right)\right]^{\frac{1}{d-1}}, \qquad \chi < -L \\ u_{h,+}(\chi) &= \left[\frac{\alpha_1(d+1)}{2\gamma_1}\operatorname{sech}^2\left(\frac{d-1}{2}\sqrt{\alpha_1}(\chi + \operatorname{sign}(p_{in})x_*)\right)\right]^{\frac{1}{d-1}}, \qquad \chi > L, \end{aligned} \tag{3.25}$$

where $x_* > 0$ is chosen such that $u_{h,\pm}(\chi = \pm L) = u_{in}$.

We denote the segments of the pinned pulse within the heterogeneous region ($|\chi| < L$) by $u_{i,\pm}(\chi, h)$, which are the solutions to

$$\begin{cases} u_\chi = p, \\ p_\chi = \alpha_2 u - \gamma_2 u^d, \\ (u,p)(0) = (u_0(h), p_0(h)), \\ (u,p)(\pm L) = (u_{in}(h), \mp p_{in}(h)). \end{cases} \tag{3.26}$$

If $u_{i,\pm}(\chi, h)$ are the homoclinic orbits of the 2nd system, then their expressions are given by

$$\begin{aligned} u_{i,-}(\chi, 0) &= \left[\frac{\alpha_2(d+1)}{2\gamma_2}\operatorname{sech}^2\left(\frac{d-1}{2}\sqrt{\alpha_2}(\chi - \operatorname{sign}(\sigma)y_*)\right)\right]^{\frac{1}{d-1}}, \qquad -L < \chi < 0, \\ u_{i,+}(\chi, 0) &= \left[\frac{\alpha_2(d+1)}{2\gamma_2}\operatorname{sech}^2\left(\frac{d-1}{2}\sqrt{\alpha_2}(\chi + \operatorname{sign}(\sigma)y_*)\right)\right]^{\frac{1}{d-1}}, \qquad 0 < \chi < L, \end{aligned} \tag{3.27}$$

where the constant $y_* > 0$ is determined by the matching condition

$$u_{h,-}(0) = \left[\frac{\alpha_2(d+1)}{2\gamma_2}\operatorname{sech}^2\left(\frac{d-1}{2}\sqrt{\alpha_2}\cdot\operatorname{sign}(\sigma)y_*\right)\right]^{\frac{1}{d-1}} = u_0. \tag{3.28}$$

As a result, equation (3.8) reduces to the algebraic relation

$$1 - \frac{2(\gamma_1 - \gamma_2)}{(d+1)(\alpha_1 - \alpha_2)}u_{in}^{d-1} = 0, \tag{3.29}$$

https://doi.org/10.1017/S0956792525100132 Published online by Cambridge University Press

which admits a unique positive solution

$$u_{in}(h=0)=\left[\frac{(d+1)(\alpha_1-\alpha_2)}{2(\gamma_1-\gamma_2)}\right]^{\frac{1}{d-1}} \tag{3.30}$$

provided $\text{sign}(\gamma_1-\gamma_2)=\text{sign}(\alpha_1-\alpha_2)$.

Theorem 4. *Let $\varepsilon>0$ be sufficiently small, and let the parameters $\alpha_1,\alpha_2>0$, $\gamma_1,\gamma_2>0$, $d>1$, $\sigma>0$ and $L>0$ be given. Suppose that equations (3.8) and (3.9) admit non-degenerate solutions $(u_{in}(h),p_{in}(h))$ and $(u_0(h),p_0(h))$, respectively, with $u_0>u_{in}$, then the following statements hold:*

- ***When*** $p_{in}>0$.
  - *If*

$$\int_{u_{in}}^{u_0}\frac{du}{\sqrt{2h+\alpha_2u^2-\frac{2\gamma_2}{d+1}u^{d+1}}}=L \tag{3.31}$$

  admits a non-degenerate root $h>0$, then system (3.1) admits a pinned pulse solution shown in Figure 3a, b.
  - *If*

$$\int_{u_{in}}^{u_0}\frac{du}{\sqrt{2h+\alpha_2u^2-\frac{2\gamma_2}{d+1}u^{d+1}}}=L\pmod T \tag{3.32}$$

  admits a non-degenerate root $h<0$, where

$$T:=\int_{u_l}^{u_r}\frac{1}{\sqrt{\alpha_2u^2-\frac{2\gamma_2}{d+1}u^{d+1}+2h}}du,$$

  in which u_l and u_r are the intersections of the periodic orbit of the 2nd system with the u-axis, then system (3.1) admits a pinned $\left(2\left\lfloor\frac{L}{T}\right\rfloor+1\right)$-hump pulse solution shown in Figure 3c.
- ***When*** $p_{in}<0$.
  - *If*

$$\int_{u_l}^{u_{in}}\frac{du}{\sqrt{2h+\alpha_2u^2-\frac{2\gamma_2}{d+1}u^{d+1}}}+\int_{u_l}^{u_0}\frac{du}{\sqrt{2h+\alpha_2u^2-\frac{2\gamma_2}{d+1}u^{d+1}}}=L\pmod T, \tag{3.33}$$

  admits a non-degenerate root $h<0$, then system (3.1) admits a pinned $\left(\left\lfloor\frac{L}{2T}\right\rfloor+3\right)$-hump pulse solution shown in Figure 3d.

Furthermore, to leading order, the pinned pulse $\left(u_h(\xi),v_h(\xi)\right)$ is given by

$$u_{p,0}(\xi)=\begin{cases}u_{0,-}(\varepsilon^2\xi), & \xi\in I_s^-,\\ u_0, & \xi\in I_f,\\ u_{0,+}(\varepsilon^2\xi), & \xi\in I_s^+,\end{cases}\qquad v_{h,0}(\xi)=\begin{cases}0, & \xi\in I_s^-,\\ v_0(\xi), & \xi\in I_f,\\ 0, & \xi\in I_s^+,\end{cases} \tag{3.34}$$

where $v_0(\xi)$ is defined by (3.4), u_0 is solved from (3.9) and

$$u_{0,-}(\chi)=\begin{cases}u_{h,-}(\chi), & \chi<-L,\\ u_{i,-}(\chi), & -L<\chi<0,\end{cases}\qquad u_{0,+}(\chi)=\begin{cases}u_{h,+}(\chi), & \chi>L,\\ u_{i,+}(\chi), & 0<\chi<L,\end{cases} \tag{3.35}$$

where $u_{h,\pm}(\chi)$ and $u_{i,\pm}(\chi,h)$ are defined in (3.25) and (3.26), respectively.

https://doi.org/10.1017/S0956792525100132 Published online by Cambridge University Press

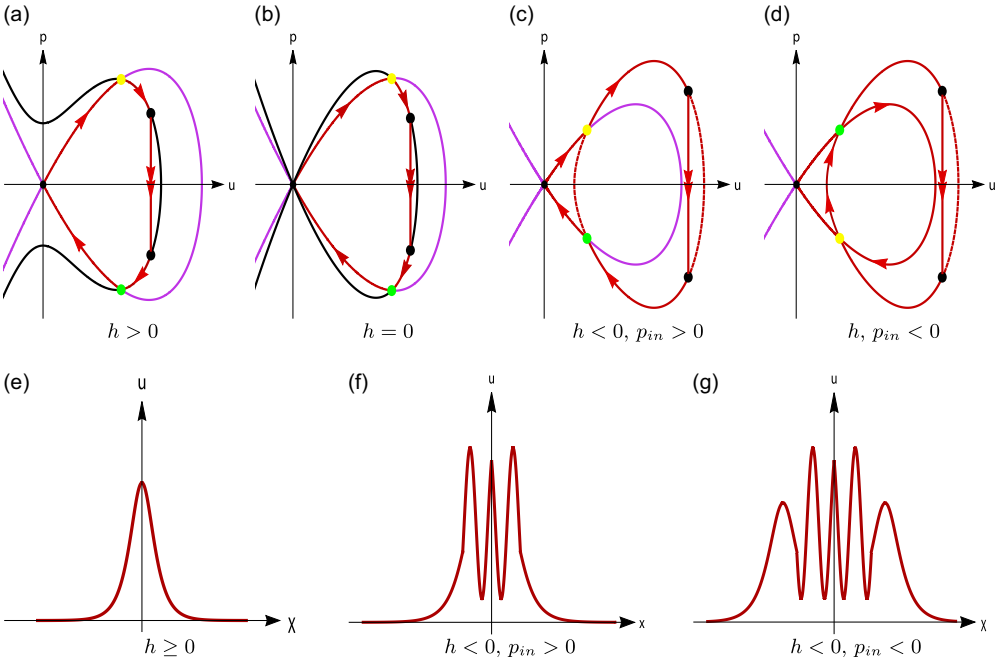

Figure 3. *(a)–(d) Sketched plots on the different types of pinned pulses $u_{p,0}(\chi)$ in the (u, p) plane, where $\sigma > 0$ and $u_0 > u_{in}$. (a) The homoclinic orbit of the 1st system connects to the open orbit of the 2nd system defined by the energy level $H = h$ $(h > 0)$. (b) The homoclinic orbits of 1st system connects to the homoclinic orbit of the 2nd system defined by $H = h$ $(h = 0)$. (c) The homoclinic orbits of 1st system connects to the periodic orbit of the 2nd system defined by $H = h$ $(h < 0)$ with $p_{in} > 0$. (d) The homoclinic orbits of 1st system connects to the periodic orbit the 2nd system defined by $H = h$ $(h < 0)$ with $p_{in} < 0$. (e)–(g) Singular pulse orbits $u_{p,0}(\chi)$ in the (χ, u) plane, in which (f) $\lfloor \frac{L}{T} \rfloor = 1$, (g) $\lfloor \frac{L}{2T} \rfloor = 1$.*

Remark 9. Theorem 4 establishes the existence of pinned pulse solutions for equation (3.1), where $\sigma > 0$ and $u_0 > u_{in}$ are fixed. As mentioned above, the sign of σ determines the direction of the fast orbit. So in a similar way, we can derive the conditions on the existence of pinned pulse solutions when $\sigma < 0$ as shown in Figure 4.

Remark 10. By comparing with the autonomous case, that is, $f(\chi) \equiv \alpha_1$ and $g(\chi) \equiv \beta_1$ in equation (3.1), which had been studied in Veerman and Doelman [37], where

$$\begin{aligned} u_{h,-}(\chi) &= \left[\frac{\alpha_1(d+1)}{2\gamma_1}\operatorname{sech}^2\left(\frac{d-1}{2}\sqrt{\alpha_1}(\chi - \operatorname{sign}(\sigma)x_*)\right)\right]^{\frac{1}{d-1}}, \qquad \chi < 0, \\ u_{h,+}(\chi) &= \left[\frac{\alpha_1(d+1)}{2\gamma_1}\operatorname{sech}^2\left(\frac{d-1}{2}\sqrt{\alpha_1}(\chi + \operatorname{sign}(\sigma)x_*)\right)\right]^{\frac{1}{d-1}}, \qquad \chi > 0, \end{aligned} \tag{3.36}$$

satisfy $u_{h,\pm}(0) = u_0$, the existence results in [37, Theorem 2.1] can be reproduced if we set $L = 0$ and $h = 0$ in Theorem 4 and Remark 9. This comparison demonstrates the validity of the results in this paper.

4. Proof of Theorem 2

In the previous section, we prove the existence of pinned pulse solutions $(u_h(x), v_h(x))$ to system (1.2). In this section, we analyse the (in)stability of these solutions.

https://doi.org/10.1017/S0956792525100132 Published online by Cambridge University Press

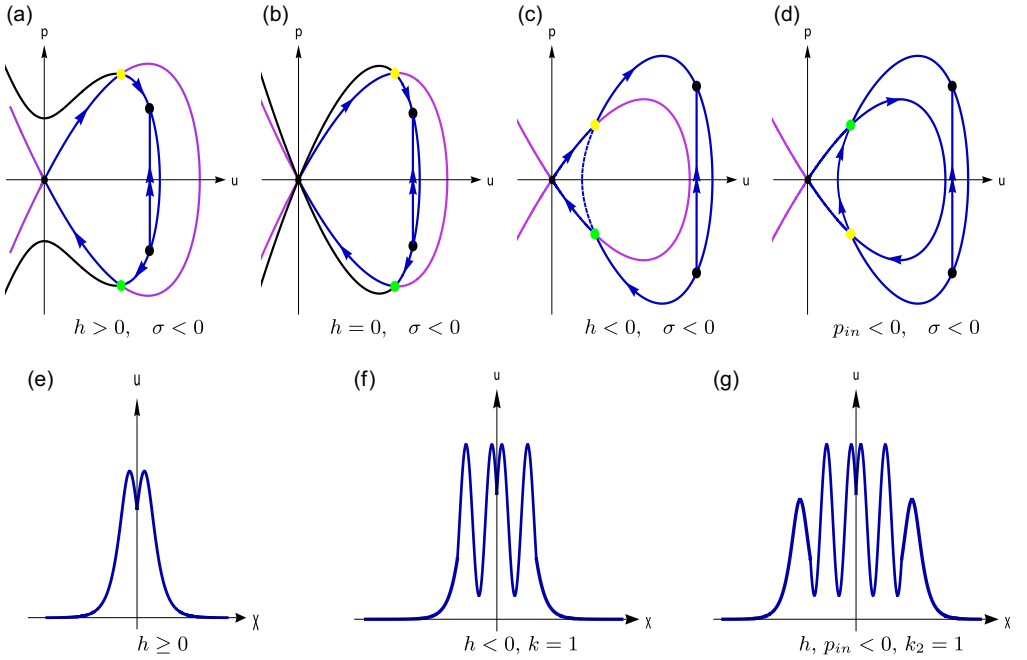

Figure 4. *(a)–(d) Sketched plots on the pinned singular homoclinic orbits $u_{p,0}(\chi)$ in the (u, p) plane with $\sigma < 0$ and $u_0 > u_{in}$. (e)–(g) Sketched plots on the pinned singular homoclinic orbits in the (χ, u) plane.*

Linearising equation (1.2) around $(u_h(x), v_h(x))$ yields

$$\begin{aligned} 0 &= \bar{u}_{xx} - \left(\varepsilon^2 \frac{\partial^2}{\partial u^2} W(u_h(x), \chi) - F_u(u_h(x), v_h(x))\right) \bar{u} + F_v(u_h(x), v_h(x))\bar{v}, \\ 0 &= \varepsilon^2 \bar{v}_{xx} - G_u(u_h(x), v_h(x), \varepsilon)\bar{u} - G_v(u_h(x), v_h(x), \varepsilon)\bar{v}. \end{aligned} \tag{4.1}$$

Then introducing the linear operator $\mathcal{L}$ gives the associated eigenvalue problem,

$$\mathcal{L}\begin{pmatrix} \bar{u} \\ \bar{v} \end{pmatrix} = \lambda \begin{pmatrix} \varepsilon^2 \bar{u} \\ \bar{v} \end{pmatrix}. \tag{4.2}$$

In terms of the fast scale $\xi = x/\varepsilon$, the eigenvalue problem turns out to be

$$\begin{aligned} \bar{u}_{\xi\xi} &= \left[\varepsilon^4 \left(\frac{\partial^2}{\partial u^2} W(u_h(\xi), \chi) + \lambda\right) + \varepsilon^2 F_u(u_h(\xi), v_h(\xi))\right] \bar{u} + \varepsilon^2 F_v(u_h(\xi), v_h(\xi))\bar{v}, \\ \bar{v}_{\xi\xi} &= G_u(u_h(\xi), v_h(\xi), \varepsilon)\bar{u} + \big(\lambda + G_v(u_h(\xi), v_h(\xi), \varepsilon)\big)\bar{v}. \end{aligned} \tag{4.3}$$

Denote $\varphi(\xi) = (\bar{u}(\xi),\ \bar{p}(\xi),\ \bar{v}(\xi),\ \bar{q}(\xi))^T$, then system (4.3) can be rewritten as

$$\varphi' = A(\xi, \lambda, \varepsilon)\varphi, \tag{4.4}$$

where

$$A(\xi, \lambda, \varepsilon) = \begin{pmatrix} 0 & \varepsilon & 0 & 0 \\ Q(\xi, \lambda, \varepsilon) & 0 & 0 & \varepsilon F_v(u_h(\xi), v_h(\xi)) \\ 0 & 0 & 0 & 1 \\ G_u(u_h(\xi), v_h(\xi), \varepsilon) & 0 & \lambda + G_v(u_h(\xi), v_h(\xi), \varepsilon) & 0 \end{pmatrix} \tag{4.5}$$

https://doi.org/10.1017/S0956792525100132 Published online by Cambridge University Press

with

$$Q(\xi,\lambda,\varepsilon)=\varepsilon^3\left(\frac{\partial^2}{\partial u^2}W(u_h(\xi),\chi)+\lambda\right)+\varepsilon F_u(u_h(\xi),v_h(\xi)).$$

This section aims to determine the spectrum $\sigma(\mathcal{L})$, which consists of the essential spectrum $\sigma_{\text{ess}}(\mathcal{L})$ and the point spectrum $\sigma_{\text{pt}}(\mathcal{L})$. According to [20, Theorem 3.1.11], the essential spectrum consists of all the eigenvalues such that the asymptotic matrix of (4.3) is not hyperbolic. Taking the limit $|\xi|\to\infty$ in $A(\xi,\lambda,\varepsilon)$, we obtain the asymptotic matrix,

$$A_\infty(\lambda,\varepsilon)=\begin{pmatrix}0 & \varepsilon & 0 & 0\\ \varepsilon^3(W_1''(0)+\lambda) & 0 & 0 & 0\\ 0 & 0 & 0 & 1\\ 0 & 0 & G_v(0,0,\varepsilon)+\lambda & 0\end{pmatrix}. \tag{4.6}$$

Solving $\det|\Lambda I-A_\infty(\lambda,\varepsilon)|=0$ gives the eigenvalues $\Lambda_{1,4}(\lambda)=\pm\Lambda_f(\lambda)$ and $\Lambda_{2,3}(\lambda)=\pm\varepsilon^2\Lambda_s(\lambda)$, where

$$\Lambda_f(\lambda)=\sqrt{G_v(0,0,\varepsilon)+\lambda},\qquad \Lambda_s(\lambda)=\sqrt{W_1''(0)+\lambda}, \tag{4.7}$$

and the corresponding eigenvectors are

$$Y_{1,4}(\lambda)=\left(0,\ 0,\ 1,\ \pm\Lambda_f(\lambda)\right)^T,\quad Y_{2,3}(\lambda)=(1,\ \pm\varepsilon\Lambda_s(\lambda),\ 0,\ 0)^T. \tag{4.8}$$

Thus, the essential spectrum of the eigenvalue problem (4.4) is

$$\Sigma_{\text{ess}}(\mathcal{L})=\left\{\lambda\in\mathbb{C}\mid\lambda\in(-\infty,-\min\{G_v(0,0,\varepsilon),W_1''(0)\}\ ]\right\}. \tag{4.9}$$

Under the assumptions (A1) and (A3), the essential spectrum lies entirely in the left half of the complex plane.

4.1. The Evans function

Define the complement of the essential spectrum in the complex plane $\mathbb{C}$ by

$$\mathcal{C}_e:=\mathbb{C}\backslash\Sigma_{\text{ess}}(\mathcal{L}).$$

Since $|\Lambda_{2,3}(\lambda)|\ll|\Lambda_{1,4}(\lambda)|$, the solutions to the eigenvalue problem (4.3) also exhibit a slow-fast nature.

Lemma 1. *For any $\lambda\in\mathcal{C}_e$, system (4.3) has four solutions $\{\varphi_{\pm,v}(\xi,\lambda),\ \varphi_{\pm,u}(\xi,\lambda)\}$ satisfying the asymptotic conditions as follows:*

$$\begin{aligned}\lim_{\xi\to-\infty}\varphi_{+,v}(\xi,\lambda)e^{-\Lambda_1(\lambda)\xi}&=Y_1(\lambda),\\ \lim_{\xi\to-\infty}\varphi_{+,u}(\xi,\lambda)e^{-\Lambda_2(\lambda)\xi}&=Y_2(\lambda),\\ \lim_{\xi\to+\infty}\varphi_{-,v}(\xi,\lambda)e^{-\Lambda_4(\lambda)\xi}&=Y_4(\lambda),\\ \lim_{\xi\to+\infty}\varphi_{-,u}(\xi,\lambda)e^{-\Lambda_3(\lambda)\xi}&=Y_3(\lambda).\end{aligned} \tag{4.10}$$

Proof. Since $A(\xi,\lambda,\varepsilon)\to A_\infty(\lambda,\varepsilon)$ as $\xi\to\pm\infty$ and

$$\int_0^{\pm\infty}\|A(\xi,\lambda,\varepsilon)-A_\infty(\lambda,\varepsilon)\|\,\mathrm{d}\xi<\infty,$$

the conclusion follows directly from [9, Theorem 4.1]. □

According to [20], λ is an eigenvalue of $\mathcal{L}$ if and only if there exists a non-trivial function $\varphi\in C^1(\mathbb{R},\mathbb{R}^4)$ solving system (4.4). By Lemma subsection 1, the solution $\varphi_{+,v/u}(\xi,\lambda)$ decays exponentially

https://doi.org/10.1017/S0956792525100132 Published online by Cambridge University Press

to $(0,0,0,0)^T$ as $\xi \to -\infty$, and $\varphi_{-,v/u}(\xi,\lambda)$ decays exponentially to $(0,0,0,0)^T$ as $\xi \to +\infty$. Thus, $\{\varphi_{+,u}, \varphi_{+,v}\}$ and $\{\varphi_{-,u}, \varphi_{-,v}\}$ span the unstable subspace $\Phi_+(\xi,\lambda)$ and the stable subspace $\Phi_-(\xi,\lambda)$, respectively. The eigenfunctions of (4.4) correspond to the intersections of these subspaces. This geometric viewpoint provides the motivation for the construction of the Evans function $E(\lambda,\varepsilon)$, which is analytic in λ, and whose zeros correspond to the eigenvalues of $\mathcal{L}$ (counted with multiplicity). These observations lead to the following definition of the Evans function:

$$E(\lambda,\varepsilon) = \det\left[\varphi_{+,v}(\xi,\lambda), \varphi_{+,u}(\xi,\lambda), \varphi_{-,u}(\xi,\lambda), \varphi_{-,v}(\xi,\lambda)\right]. \tag{4.11}$$

Consequently, the problem of identifying the eigenvalues is reduced to the location the zeros of the analytic function $E(\lambda,\varepsilon)$ (see [20, Lemma 9.3.4]). Since $\Lambda_{1,4}(\lambda) = \mathcal{O}(1)$ and $\Lambda_{2,3}(\lambda) = \mathcal{O}(\varepsilon^2) \ll 1$, the functions $\varphi_{+,v}(\xi,\lambda)$ and $\varphi_{-,v}(\xi,\lambda)$ are uniquely determined by their asymptotic behaviour as $\xi \to -\infty$ and $\xi \to \infty$.

Since $v_h(\xi)$ vanishes at leading order in the slow fields, it follows that $A(\xi,\lambda,\varepsilon)$ approaches a slowly varying intermediate matrix, namely,

$$A_s(\xi,\lambda,\varepsilon) = \begin{pmatrix} 0 & \varepsilon & 0 & 0 \\ \varepsilon^3\left(\dfrac{\partial^2}{\partial u^2}W(u_{p,0}(\xi),\varepsilon^2\xi)+\lambda\right) & 0 & 0 & 0 \\ 0 & 0 & 0 & 1 \\ 0 & 0 & G_v(u_{p,0}(\xi),0,0)+\lambda & 0 \end{pmatrix}. \tag{4.12}$$

We observe in (4.12) that the dynamics of the slow and fast variables have been separated. Furthermore, the distance between $A_s(\xi,\lambda,\varepsilon)$ and $A_\infty(\lambda,\varepsilon)$ is exponentially small.

Lemma 2. *Consider*

$$\frac{d}{d\xi}\psi = A_s(\xi,\lambda,\varepsilon)\psi, \tag{4.13}$$

where $\psi = (u,p,v,q)^T$ and $A_s(\xi,\lambda,\varepsilon)$ is given in (4.12). Let $\lambda \in \Omega$, and then for $\xi < -\frac{1}{\sqrt{\varepsilon}}$, the stable and unstable subspaces of (4.13) are, respectively, spanned by $\psi^-_{+,u,v}(\xi,\lambda)$ and $\psi^-_{-,u,v}(\xi,\lambda)$, which are given by

$$\psi^-_{\pm,u}(\xi,\lambda) = \left(u_\pm(\xi,\lambda), \frac{1}{\varepsilon}\frac{du_\pm}{d\xi}(\xi,\lambda), 0, 0\right)^T, \quad \psi^-_{\pm,v}(\xi,\lambda) = \left(0,0,v_\pm(\xi,\lambda), \frac{dv_\pm}{d\xi}(\xi,\lambda)\right)^T, \tag{4.14}$$

enjoying the following properties:

$$\begin{aligned} \lim_{\xi\to-\infty} \psi^-_{+,u}(\xi,\lambda)e^{-\Lambda_2(\lambda)\xi} &= Y_2(\lambda), \\ \lim_{\xi\to+\infty} \psi^-_{-,u}(\xi,\lambda)e^{-\Lambda_3(\lambda)\xi} &= Y_3(\lambda), \\ \lim_{\xi\to-\infty} \psi^-_{+,v}(\xi,\lambda)e^{-\Lambda_1(\lambda)\xi} &= Y_1(\lambda), \\ \lim_{\xi\to+\infty} \psi^-_{-,v}(\xi,\lambda)e^{-\Lambda_4(\lambda)\xi} &= Y_4(\lambda). \end{aligned} \tag{4.15}$$

For $\xi > \frac{1}{\sqrt{\varepsilon}}$, by the reversibility symmetry, the solution spaces of (4.13) now are spanned by $\psi^+_{\pm,u,v}(\xi,\lambda)$, where

$$\begin{aligned} \psi^+_{\pm,u}(\chi;\lambda) &= \left(u_\mp(-\xi;\lambda), -\frac{1}{\varepsilon}\frac{du_\mp}{d\xi}(-\xi;\lambda), 0, 0\right)^T, \\ \psi^+_{\pm,v}(\chi;\lambda) &= \left(0,0,v_\mp(-\xi;\lambda), -\frac{dv_\mp}{d\xi}(-\xi;\lambda)\right)^T. \end{aligned} \tag{4.16}$$

https://doi.org/10.1017/S0956792525100132 Published online by Cambridge University Press

Theorem 5. *The eigenvalues are given by the zeros of the Evans function*

$$E(\lambda,\varepsilon)=4\,\varepsilon t_{s,+}(\lambda,\varepsilon)t_{f,+}(\lambda,\varepsilon)\sqrt{G_v(0,0,\varepsilon)+\lambda}\sqrt{W_1''(0)+\lambda}, \tag{4.17}$$

where $t_{f,+}(\lambda,\varepsilon)$ is an analytic transmission function and $t_{s,+}(\lambda,\varepsilon)$ is meromorphic function in λ. These functions are defined via the asymptotic behaviour

$$\begin{aligned}\lim_{\xi\to+\infty}\varphi_{+,v}(\xi,\lambda)\,e^{-\Lambda_1(\lambda)\xi}&=t_{f,+}(\lambda,\varepsilon)Y_1(\lambda),\\ \lim_{\xi\to+\infty}\varphi_{+,u}(\xi,\lambda)\,e^{-\Lambda_2(\lambda)\xi}&=t_{s,+}(\lambda,\varepsilon)Y_2(\lambda),\end{aligned} \tag{4.18}$$

where $\varphi_{+,v}(\xi,\lambda)$ has been stated in Lemma subsection 1 and $\varphi_{+,u}(\xi,\lambda)$ is the unique solution to (4.4), provided $t_{f,+}(\lambda,\varepsilon)\neq 0$, satisfying the boundary conditions

$$\begin{aligned}\lim_{x\to-\infty}\varphi_{+,u}(\xi,\lambda)e^{-\Lambda_2(\lambda)\,\xi}&=Y_2(\lambda),\\ \lim_{x\to+\infty}\varphi_{+,u}(\xi,\lambda)e^{-\Lambda_1(\lambda)\xi}&=(0,0,0,0)^T.\end{aligned} \tag{4.19}$$

Moreover, there exists a meromorphic transmission function $t_{s,-}(\lambda,\varepsilon)$ such that, to leading order,

$$\varphi_{+,u}(\xi,\lambda)=\begin{cases}\psi^-_{+,u}(\xi,\lambda), & \xi<-\dfrac{1}{\sqrt{\varepsilon}},\\ t_{s,+}(\lambda,\varepsilon)\psi^-_{-,u}(-\xi,\lambda)+t_{s,-}(\lambda,\varepsilon)\psi^-_{+,u}(-\xi,\lambda), & \xi\ >\ \dfrac{1}{\sqrt{\varepsilon}}.\end{cases} \tag{4.20}$$

Proof. It follows from (3.34) that there are two positive, $\mathcal{O}(1)$ constants C_1 and C_2 such that

$$\|A(\xi,\lambda,\varepsilon)-A_s(\xi,\lambda,\varepsilon)\|\le C_1\mathrm{e}^{-C_2|\xi|}$$

for $\xi\in I_s^{\pm}$. Hence, to leading order, $\psi_{\pm,v}(\xi,\lambda)$ and $\psi_{\pm,u}(\xi,\lambda)$ can be selected as basis solutions to (4.4). According to the asymptotics of $\varphi_{+,v}(\xi,\lambda)$ as $\xi\to-\infty$, we know that it remains exponentially close to $\psi_{+,v}(\xi,\lambda)$ for $\xi<-\frac{1}{\sqrt{\varepsilon}}$. Although the exact form of $\varphi_{+,v}(\xi,\lambda)$ is unknown, to leading order, it can be written as

$$\varphi_{+,v}(\xi,\lambda)=t_{f,+}(\lambda)\psi^+_{+,v}(\xi)+t_{f,-}(\lambda)\psi^+_{-,v}(\xi)+t_+(\lambda)\psi^+_{+,u}(\xi)+t_-(\lambda)\psi^+_{-,u}(\xi)$$

for $\xi>\frac{1}{\sqrt{\varepsilon}}$. This proves the first result in (4.18). In order to determine $\varphi_{+,u}(\xi)$ uniquely, it can be found that $\varphi_{+,u}(\xi,\lambda)$ grows obeying the speed of $\mathcal{O}(\mathrm{e}^{\Lambda_2(\lambda)\,\xi})$. That is, $\varphi_{+,u}(\xi,\lambda)$ must satisfy (4.19) if $t_{f,+}(\lambda)\neq 0$. Hence, similar to $\varphi_{+,v}(\xi,\lambda)$, we obtain (4.20) accordingly.

By Liouville's formula and $\mathrm{TrA}(x)=\Sigma_{i=1}^4\Lambda_i(\lambda)$, the Evans function turns out to be

$$\begin{aligned}E(\lambda,\varepsilon)&=\lim_{\xi\to+\infty}\det\left[\varphi_{+,v}(\xi,\lambda),\varphi_{+,u}(\xi,\lambda),\varphi_{-,u}(\xi,\lambda),\varphi_{-,v}(\xi,\lambda)\right]e^{-\int_0^x TrA(x)dx}\\ &=\lim_{\xi\to+\infty}\det\left[\varphi_{+,v}(\xi,\lambda)e^{-\Lambda_1(\lambda)\xi},\varphi_{+,u}(\xi,\lambda)e^{-\Lambda_2(\lambda)\xi},\varphi_{-,u}(\xi,\lambda)e^{-\Lambda_3(\lambda)\xi},\varphi_{-,v}(\xi,\lambda)e^{-\Lambda_4(\lambda)\xi}\right]\\ &=\det\left[t_{f,+}(\lambda,\varepsilon)Y_1(\lambda),t_{s,+}(\lambda,\varepsilon)Y_2(\lambda),Y_3(\lambda),Y_4(\lambda)\right]\\ &=4\varepsilon t_{s,+}(\lambda,\varepsilon)t_{f,+}(\lambda,\varepsilon)\sqrt{G_v(0,0,\varepsilon)+\lambda}\sqrt{W_1''(0)+\lambda}.\end{aligned}$$

□

As a consequence, the eigenvalues of (4.3) are exactly identical with the roots of $t_{s,+}(\lambda,\varepsilon)$ or $t_{f,+}(\lambda,\varepsilon)$. Nevertheless, we will also see that some roots of $t_{f,+}(\lambda,\varepsilon)$ may not correspond to the true eigenvalues, as $t_{s,+}(\lambda,\varepsilon)$ may possess poles at these values, which cancel the zeros.

4.2. The fast transmission function $t_{f,+}(\lambda,\varepsilon)$

In this section, we determine the zeros of the fast transmission function $t_{f,+}(\lambda,\varepsilon)$.

https://doi.org/10.1017/S0956792525100132 Published online by Cambridge University Press

Let $\varepsilon \to 0$ in system (4.3), we get

$$(\mathcal{L}_f - \lambda)v = G_u(u_0, v_0(\xi), 0)\,\bar{u}(0), \qquad \mathcal{L}_f v{:}v_{\xi\xi} - G_v(u_0, v_0(\xi), 0)\,v, \tag{4.21}$$

which is a second-order inhomogeneous differential equation. Here, we have used the fact that $u_h(\xi) = u_0$ and $v_h(\xi) = v_0(\xi)$ for $\xi \in I_f$ as $\varepsilon \to 0$. Equation (4.21) corresponds to the fast limiting eigenvalue problem in the singular limit of system (4.3), which is a classical Sturm–Liouville eigenvalue problem. Thus, by Sturm–Liouville theory, the eigenvalues of $\mathcal{L}_f$ can be enumerated in a strictly descending order,

$$\lambda_0^f > \lambda_1^f = 0 > \cdots > \lambda_N^f > -G_v(u_0, 0, 0).$$

Moreover, the eigenfunction $\bar{v}_i(\xi)$ corresponding to λ_i^f has exactly i distinct zeroes and is even or odd depending on whether i is even or odd, respectively.

The homogeneous problem associated with system (4.21) can be written as

$$\frac{\mathrm{d}}{\mathrm{d}\xi}\phi = A_f(\xi, \lambda)\phi, \tag{4.22}$$

where $\phi = (v, q)^T$ and $A_f(\xi, \lambda)$ is a 2×2 matrix, which is exactly the lower 2×2 block of $A(\xi, \lambda, \varepsilon)$ in the limit $\varepsilon \to 0$. Obviously, system (4.22) has two solutions $\phi_+(\xi, \lambda)$, $\phi_-(\xi, \lambda)$ satisfying

$$\lim_{\xi \to -\infty} \phi_+(\xi, \lambda)e^{-\Lambda_1(\lambda)\xi} = (1, \Lambda_1(\lambda))^T, \qquad \lim_{\xi \to +\infty} \phi_-(\xi, \lambda)e^{-\Lambda_4(\lambda)\xi} = (1, \Lambda_4(\lambda))^T, \tag{4.23}$$

and there exists an analytic function $t_f(\lambda)$ such that

$$\lim_{\xi \to +\infty} \phi_+(\xi, \lambda)e^{-\Lambda_1(\lambda)\xi} = t_f(\lambda)(1, \Lambda_1(\lambda))^T. \tag{4.24}$$

The Evans function associated with this problem is given by

$$E_f(\lambda) = \lim_{\xi \to +\infty} \det\left[\phi_+(\xi, \lambda), \phi_-(\xi, \lambda)\right] = \det\left[t_f(\lambda)(1, \Lambda_1(\lambda))^T, (1, \Lambda_4(\lambda))^T\right] = -2t_f(\lambda)\Lambda_1(\lambda). \tag{4.25}$$

By construction, the leading order behaviour of $t_{f,+}(\lambda, \varepsilon)$ is determined by $t_f(\lambda)$. It thus follows from (4.25) that $t_f(\lambda) = 0$ if and only if $E_f(\lambda) = 0$. Hence, the eigenvalues of (4.22) correspond to the zeros of $t_f(\lambda) = 0$. That is, the roots of the function $t_f(\lambda)$ are given by λ_i^f, $i = 0, 1, \ldots, N$.

Lemma 3. *Let $0 < \varepsilon \ll 1$, then the fast transmission function is given by*

$$t_{f,+}(\lambda, \varepsilon) = \tilde{t}_f(\lambda, \varepsilon) \prod_{i=1}^{n} \left(\lambda - \lambda_i^f(\varepsilon)\right) \tag{4.26}$$

with $\tilde{t}_f(\lambda, \varepsilon) \neq 0$, and $\lambda_i^f(\varepsilon)$ has the following regular expansion:

$$\lambda_i^f(\varepsilon) = \lambda_i^f + \varepsilon^2 \lambda_{i,1}^f + \mathcal{O}(\varepsilon^4), \tag{4.27}$$

for $i = 0, 1, \ldots, N$.

The proof of this lemma is analogous to those in [12–14] by using the 'elephant trunk' procedure [1, 18]. It is important to note that $\lambda_1^f(\varepsilon) \equiv 0$ is no longer valid since system (1.2) now is non-autonomous, leading to the loss of translational invariance. As a result, under the perturbation, the eigenvalue $\lambda_1^f(\varepsilon)$ may be shifted to the one having the positive real part. Under certain situations, standard perturbation methods such as the Lin–Sandstede method [3, 20, 23] can be applied to estimate the location of these eigenvalues. However, due to the piecewise-smooth nature of system (1.2), no effective methods currently exist for precisely determining the location of these eigenvalues.

Remark 11. While the Lin–Sandstede method can be used to detect the eigenvalue bifurcating from $\lambda = 0$ under perturbations, its validity depends heavily on the assumption that the eigenfunction associated with the perturbed eigenvalue remains a small deformation of the unperturbed one. This assumption enables a regular perturbation approach, where a solvability condition – typically of Fredholm type – is imposed to determine the first-order correction $\lambda = \lambda_1^f(\varepsilon)$. However, in the singularly perturbed system studied here, this assumption does not hold. As shown in the previous section, the pulse solution undergoes a transition when it passes the interfaces at $\chi = \pm L$. Consequently, the eigenfunction associated

https://doi.org/10.1017/S0956792525100132 Published online by Cambridge University Press

with $\lambda = \lambda_1^f(\varepsilon)$ does not converge to the eigenfunction associated with $\lambda = 0$ as $\varepsilon \to 0$. So Lin–Sandstede method is not applicable here. We adopt an alternative technique to study the spectrum of the linearised operator.

Although $\lambda_0^f(\varepsilon)$ is a simple zero of the function $t_{f,+}(\lambda, \varepsilon)$, this does not imply that the function $E(\lambda, \varepsilon)$ also vanishes at this point. This is due to the fact that $\lambda = \lambda_0^f(\varepsilon)$ is a first-order pole of the transmission function $t_{s,+}(\lambda)$ and therefore cannot be an eigenvalue of the full system. This phenomenon is known as the 'NLEP Paradox' in literature.

According to (4.23)–(4.24), we know that $\phi_+(\xi, \lambda)$ and $\phi_-(\xi, \lambda)$ form a fundamental set of linearly independent solutions to the homogeneous system (4.22) for $\lambda \neq \lambda_i^f$, $i = 0, 1, \ldots N$. Consequently, by employing the method of constant variation we can derive a bounded solution to the heterogeneous problem (4.21).

Lemma 4. *For $\lambda \neq \lambda_i^f$, $i = 0, 1, \ldots N$, the unique bounded solution $v_{in}(\xi, \lambda)$ to the inhomogeneous problem (4.21) is given by*

$$\begin{aligned} v_{in}(\xi, \lambda) = \frac{\bar{u}(0)}{E_f(\lambda)} \Bigg(& v_-(\xi, \lambda) \int_{-\infty}^{\xi} G_u(u_0, v_0(s), 0) v_+(s, \lambda)\, ds \\ & + v_+(\xi, \lambda) \int_{\xi}^{+\infty} G_u(u_0, v_0(s), 0) v_-(s, \lambda)\, ds \Bigg), \end{aligned} \tag{4.28}$$

where $v_\pm(\xi, \lambda)$ is the v-component of $\phi_\pm(\xi, \lambda) = (v_\pm(\xi, \lambda), q_\pm(\xi, \lambda))$, and $E_f(\lambda)$ is defined as in (4.25).

Lemma 5. *(See [10]) The bounded solution $v_{in}(\xi, \cdot)$ is meromorphic in the region $\mathcal{C}_e$ for fixed $\xi \in \mathbb{R}$ and analytic on $\mathcal{C}_e \backslash \{\lambda_i^f\}_{i=0}^N$ for $\xi \in \mathbb{R}$. Furthermore, when i is even, $\lambda = \lambda_i^f$ is a pole of $v_{in}(\xi, \lambda)$, while when i is odd, it is a removable singularity.*

Proof. Since $\mathcal{L}_f - \lambda$ is a Fredholm operator of index zero for $\lambda \in \mathcal{C}_e$, and $\mathcal{L}_f - \lambda$ is invertible if and only if $\lambda \in \mathcal{C}_e \backslash \{\lambda_i^f\}_{i=0}^N$, it follows that $(\mathcal{L}_f - \lambda)^{-1}$ is analytic on $\mathcal{C}_e \backslash \{\lambda_i^f\}_{i=0}^N$ and meromorphic on the entire region $\mathcal{C}_e$. Since $\mathcal{L}_f - \lambda$ is a self-adjoint operator, it follows from the Fredholm alternative [20, Theorem 2.2.1] that a bounded solution to the inhomogeneous equation exists at $\lambda \in \{\lambda_i^f\}_{i=0}^N$ if and only if the following solvability condition is satisfied:

$$\int_{-\infty}^{+\infty} G_u(u_0, v_0(\xi), 0) \bar{v}_i(\xi, \lambda)\, \mathrm{d}\xi = 0,$$

where $\bar{v}_i(\xi, \lambda) \in \ker(\mathcal{L}_f - \lambda)$. According to Sturm–Liouville theory, if i is even, the corresponding eigenfunction $\bar{v}_i(\xi)$ is an even function, and if i is odd, it is an odd function. Since the homoclinic solution $v_0(\xi)$ is even, the solvability condition does not hold when i is even. Therefore, $\lambda = \lambda_i^f$ is a pole of $v_{in}(\xi, \lambda)$. When i is odd, the solvability condition holds, and $\lambda = \lambda_i^f$ is a removable singularity. □

Remark 12. The bounded solution $v_{in}(\xi, \lambda)$ to the inhomogeneous problem (4.21) forms one of the key ingredients of the slow transmission function $t_{s,+}(\lambda, \varepsilon)$ (see the subsequent subsection).

4.3. The slow transmission function $t_{s,+}(\lambda, \varepsilon)$

We will see that the slow transmission function $t_{s,+}(\lambda, \varepsilon)$ can be determined by matching the slow and fast orbits, respectively, of the following slow limit eigenvalue problem:

$$\begin{cases} u_\chi = p, \\ p_\chi = \big(W(u_{p,0}(\chi), \chi) + \lambda\big)\, u, \end{cases} \tag{4.29}$$

and the fast limit eigenvalue problem (4.21).

https://doi.org/10.1017/S0956792525100132 Published online by Cambridge University Press

Recall that, on the slow intervals $I_s^{\pm}$,

$$\psi_{\pm,u}^{+}(\xi,\lambda)=\left(u_{\pm}(\xi,\lambda),\frac{1}{\varepsilon}\frac{du_{\pm}}{d\xi}(\xi,\lambda),0,0\right).$$

To simplify the notation and to enhance the clarity of formulation, we utilise the variable $\chi=\varepsilon^2\xi$ and define $(u_{\pm}(\chi,\lambda),p_{\pm}(\chi,\lambda))$.

Denote

$$\psi_{\pm,u}^{+}(\chi,\lambda)=(u_{\pm}(\chi,\lambda),\varepsilon p_{\pm}(\chi,\lambda),0,0)$$

with $p_{\pm}(\chi,\lambda)=\frac{\mathrm{d}}{\mathrm{d}\chi}u_{\pm}(\chi,\lambda)$; thus, $(u_{\pm}(\chi,\lambda),p_{\pm}(\chi,\lambda))$ is the unique solution to the slow limit eigenvalue problem (4.29) satisfying

$$\lim_{\chi\to\mp\infty}(u_{\pm}(\chi,\lambda),p_{\pm}(\chi,\lambda))\mathrm{e}^{\mp\Lambda_s(\lambda)\chi}=(1,\ \pm\Lambda_s(\lambda)).$$

Lemma 6. *Define $u_{\pm}(0,\lambda)=u_{\pm}(\chi=0)$ and $p_{\pm}(0,\lambda)=p_{\pm}(\chi=0)$, then the leading order of the slow transmission function can be given by*

$$t_{s,+}(\lambda)=-\frac{\Big(u_{+}(0,\lambda)\mathcal{G}(\lambda)+2p_{+}(0,\lambda)\Big)u_{+}(0,\lambda)}{u_{+}(0,\lambda)p_{-}(0,\lambda)-u_{-}(0,\lambda)p_{+}(0,\lambda)},\tag{4.30}$$

where

$$\mathcal{G}(\lambda)=\int_{-\infty}^{+\infty}\int_{-\infty}^{\xi}\left(F_u(u_0,v_0(\xi)+\frac{F_v(u_0,v_0(\xi))}{E_f(\lambda)}G_u(u_0,v_0(s),0)v_{+}(s,\lambda)v_{-}(\xi,\lambda)\right)ds\,d\xi.\tag{4.31}$$

Proof. It follows from Theorem 5 that there exists a positive constant K independent of ε such that

$$\varphi_{+,u}(\xi,\lambda)=\psi_{+,u}^{-}(\xi,\lambda)+\mathcal{O}(e^{-K\xi}),$$

for $\xi\in I_s^{-}$, and

$$\varphi_{+,u}(\xi,\lambda)=t_{s,+}(\lambda,\varepsilon)\psi_{+,u}^{+}(\xi,\lambda)+t_{s,-}(\lambda,\varepsilon)\psi_{-,u}^{+}(\xi,\lambda)+\mathcal{O}(e^{-K\xi})$$

for $\xi\in I_s^{+}$. Accordingly, we can determine the explicit representation of $t_{s,+}(\lambda,\varepsilon)$ by matching the fast and slow orbits. More precisely, to compute $t_{s,+}(\lambda,\varepsilon)$, we need to track the changes of $\bar{u}_{+}(\xi,\lambda)$ and $\bar{p}_{+}(\xi,\lambda)$ during the fast transition, that is, $\xi\in I_f$.

We define the slow difference function Δ_s by

$$\Delta_s\begin{pmatrix}\bar{u}\\ \bar{p}\\ \bar{v}\\ \bar{q}\end{pmatrix}=\lim_{\xi\downarrow\frac{1}{\sqrt{\varepsilon}}}\left(t_{s,+}(\lambda,\varepsilon)\psi_{-,u}^{-}(-\xi;\lambda)+t_{s,-}(\lambda,\varepsilon)\psi_{+,u}^{-}(-\xi;\lambda)\right)-\lim_{\xi\uparrow-\frac{1}{\sqrt{\varepsilon}}}\psi_{+,u}^{-}(\xi,\lambda).\tag{4.32}$$

First, it follows from (4.4) that $\bar{u}_{+}(\xi,\lambda)$ remains constant to leading order during the fast field I_f. As a consequence,

$$\bar{u}_{+}\left(-\frac{1}{\sqrt{\varepsilon}}\right)=\bar{u}_{+}\left(\frac{1}{\sqrt{\varepsilon}}\right)+\mathcal{O}(\varepsilon^{3/2}).\tag{4.33}$$

This together with

$$\bar{u}\left(-\frac{1}{\sqrt{\varepsilon}}\right)=u_{+}(0,\lambda)+\mathcal{O}(\varepsilon^{3/2})\tag{4.34}$$

gives

$$\bar{u}\left(\frac{1}{\sqrt{\varepsilon}}\right)=t_{s,+}(\lambda)u_{-}(0,\lambda)+t_{s,-}(\lambda)u_{+}(0,\lambda)+\mathcal{O}(\varepsilon^{3/2}).\tag{4.35}$$

https://doi.org/10.1017/S0956792525100132 Published online by Cambridge University Press

Thus, the first matching condition (4.33) can be written as

$$u_+(0,\lambda) = t_{s,+}(\lambda)u_-(0,\lambda) + t_{s,-}(\lambda)u_+(0,\lambda). \tag{4.36}$$

So the first relation between $t_{s,+}(\lambda)$ and $t_{s,-}(\lambda)$ can be given by

$$t_{s,-}(\lambda) = 1 - \frac{u_-(0,\lambda)}{u_+(0,\lambda)} t_{s,+}(\lambda). \tag{4.37}$$

On the other hand, the derivative $\bar{p}_+(\xi,\lambda)$ changes rapidly in the fast field I_f. It can be determined through the following two ways. First, we use the information on $\varphi_{+,u}(\xi,\lambda)$ in the slow field to compute it. The change $\Delta_s\bar{p}$, to leading order, can be approximated by the difference of $\bar{p}_+(\xi,\lambda)$ between two ends of the slow field, that is,

$$\begin{aligned}
\Delta_s\bar{p} &= \bar{p}_+\left(\frac{1}{\sqrt{\varepsilon}}\right) - \bar{p}_+\left(-\frac{1}{\sqrt{\varepsilon}}\right) \\
&= \frac{1}{\varepsilon}\left(t_{s,+}(\lambda)\frac{\mathrm{d}}{\mathrm{d}\xi}u_-(-\xi) + t_{s,-}(\lambda)\ \frac{\mathrm{d}}{\mathrm{d}\xi}u_+(-\xi)\right)\Big|_{\xi=\frac{1}{\sqrt{\varepsilon}}} - \frac{1}{\varepsilon}\ \frac{\mathrm{d}}{\mathrm{d}\xi}u_+(\xi)\Big|_{\xi=-\frac{1}{\sqrt{\varepsilon}}} \\
&= -\frac{1}{\varepsilon}\left(t_{s,+}(\lambda)\frac{\mathrm{d}}{\mathrm{d}\xi}u_-(\xi) + t_{s,-}(\lambda)\ \frac{\mathrm{d}}{\mathrm{d}\xi}u_+(\xi) + \frac{\mathrm{d}}{\mathrm{d}\xi}u_+(\xi)\right)\Big|_{\xi=-\frac{1}{\sqrt{\varepsilon}}} \\
&= -\frac{1}{\varepsilon}\left(t_{s,+}(\lambda)\frac{\mathrm{d}}{\mathrm{d}\xi}u_-(\xi) + \left(1 - \frac{u_-(0)}{u_+(0)}t_{s,+}(\lambda)\right)\ \frac{\mathrm{d}}{\mathrm{d}\xi}u_+(\xi) + \frac{\mathrm{d}}{\mathrm{d}\xi}u_+(\xi)\right)\Big|_{\xi=-\frac{1}{\sqrt{\varepsilon}}} \\
&= -\varepsilon\left[\left(\frac{\mathrm{d}}{\mathrm{d}\chi}u_-(\chi) - \frac{u_-(0)\frac{\mathrm{d}}{\mathrm{d}\chi}u_+(\chi)}{u_+(0)}t_{s,+}(\lambda)\right) + 2\frac{\mathrm{d}}{\mathrm{d}\chi}u_+(\chi)\right]\Big|_{\chi=-\varepsilon^{3/2}} \\
&= -\varepsilon\left(\frac{u_+(0)p_-(0) - u_-(0)p_+(0)}{u_+(0)}t_{s,+}(\lambda) + 2p_+(0)\right).
\end{aligned} \tag{4.38}$$

Second, the accumulated jump concerning the first-order derivative can be obtained by integrating $\bar{u}_{\xi\xi}$ over the fast field, that is, to leading order,

$$\begin{aligned}
\Delta_f\,\bar{p} &= \frac{1}{\varepsilon}\int_{I_f}\bar{u}_{\xi\xi}\,\mathrm{d}\xi \\
&= \varepsilon\int_{-\infty}^{+\infty}\left(F_u(u_0, v_0(\xi)\bar{u}(0) + F_v(u_0, v_0(\xi))v_{in}(\xi,\lambda)\right)\mathrm{d}\xi, \\
&= \varepsilon u_+(0)\int_{-\infty}^{+\infty}\int_{-\infty}^{\xi}\left(F_u(u_0, v_0(\xi) + \frac{F_v(u_0, v_0(\xi))}{E_f(\lambda)}G_u(u_0, v_0(s), 0)v_+(s;\lambda)v_-(\xi,\lambda)\right)\mathrm{d}s\,\mathrm{d}\xi.
\end{aligned} \tag{4.39}$$

By combining (4.38) and (4.39), one can get (4.30) up to the leading order. □

Remark 13. It is worthy to note that only the roots of $t_{s,+}(\lambda,0)$ are not sufficient to decide the spectral stability of the pinned pulse of (1.2) due to the fact that the sign of $\lambda_1^f(\varepsilon)$ cannot be determined.

Remark 14. If $F_v(u,v) \equiv 0$ for all $u,\ v > 0$, then

$$\mathcal{G}(\lambda) = \int_{-\infty}^{+\infty}\int_{-\infty}^{\xi} F_u(u_0, v_0(\xi))\,\mathrm{d}s\,\mathrm{d}\xi,$$

which implies that the transmission function $t_{s,+}(\lambda,\varepsilon)$ is only determined by the slow reduced eigenvalues problem (4.29). As a consequence, $t_{s,+}(\lambda,\varepsilon)$ is analytic on $\mathcal{C}_e$, and the zeros of $t_{f,+}(\lambda,\varepsilon)$ cannot be cancelled by the poles of $t_{s,+}(\lambda,\varepsilon)$. In this case, we conclude that the linearised eigenvalue problem

https://doi.org/10.1017/S0956792525100132 Published online by Cambridge University Press

can be completely separated into the slow and fast reduced eigenvalue problems without the interaction between them. Thus, the zeros of $t_{f,+}(\lambda,\varepsilon)$ with positive real parts yield the spectral instability directly.

5. (In)stability of pinned pulses in non-autonomous GM equation

Consider

$$\begin{cases} \varepsilon^2 U_t = U_{xx} - \varepsilon^2\Big(f(\chi)U - g(\chi)U^d\Big) + \sigma V^2, \\ V_t = \varepsilon^2 V_{xx} - V + \frac{V^2}{U}, \end{cases} \tag{5.1}$$

whose existence has been set up in Section 3. The associated eigenvalue problem is

$$\varphi' = A(\xi,\lambda,\varepsilon)\varphi, \tag{5.2}$$

where $\varphi(\xi) = (\bar{u}(\xi), \bar{p}(\xi), \bar{v}(\xi), \bar{q}(\xi))^T$, and

$$A(\xi,\lambda,\varepsilon) = \begin{pmatrix} 0 & \varepsilon & 0 & 0 \\ \varepsilon^3(f(\chi) - dg(\chi)u_h^{d-1}(\varepsilon^2\xi) + \lambda) & 0 & -2\varepsilon\sigma v_h(\xi) & 0 \\ 0 & 0 & 0 & 1 \\ \dfrac{v_h^2(\xi)}{u_h^2(\varepsilon^2\xi)} & 0 & 1+\lambda - \dfrac{2v_h^2(\xi)}{u_h(\varepsilon^2\xi)} & 0 \end{pmatrix}. \tag{5.3}$$

By (5.2), the essential spectrum turns out to be

$$\Sigma_{ess} = \{\lambda \in \mathbb{C} \mid \lambda \in (-\infty, -\min\{1, \alpha_1\}]\}. \tag{5.4}$$

Now (4.21) becomes

$$(\mathcal{L}_f - \lambda)v = \frac{v_0^2(\xi)}{u_0^2}\bar{u}(0), \qquad \mathcal{L}_f v := v_{\xi\xi} - \left(1 - \frac{2v_0(\xi)}{u_0}\right)v. \tag{5.5}$$

Obviously, the eigenvalues associated with the operator $\mathcal{L}_f$ are well-known, namely, $\lambda_0^f = 5/4$, $\lambda_1^f = 0$ and $\lambda_2^f = -3/4$.

As treated in [37], we can obtain the following result.

Lemma 7. *For $0 < \varepsilon \ll 1$, the fast transmission function can be given by*

$$t_{f,+}(\lambda,\varepsilon) = \tilde{t}_f(\lambda,\varepsilon)\left(\lambda - \lambda_0^f(\varepsilon)\right)\left(\lambda - \lambda_1^f(\varepsilon)\right)\left(\lambda - \lambda_2^f(\varepsilon)\right) \tag{5.6}$$

with $\tilde{t}_f(\lambda,\varepsilon) \neq 0$, and $\lambda_i^f(\varepsilon)$ has the following regular expansion:

$$\lambda_i^f(\varepsilon) = \lambda_i^f + \varepsilon^2\lambda_{i,1}^f + \mathcal{O}(\varepsilon^4), \quad i = 0, 1, 2. \tag{5.7}$$

In particular, for $\lambda \neq \lambda_i^f$, $i = 0, 1, 2$, the unique solution of $v_{in}(\xi,\lambda)$ to the heterogeneous problem (4.21) now is

$$v_{in}(\zeta,\lambda) = 9\bar{u}(0)\Big[v_+(\zeta,\lambda)\int_{-1}^{\zeta}(1-s^2)v_-(s,\lambda)\,ds + v_-(\zeta,\lambda)\int_{-1}^{\zeta}(1-s^2)v_+(s,\lambda)\,ds\Big], \tag{5.8}$$

where $v_\pm(\zeta,\lambda) = c_\pm(\lambda)P_3^{-2\sqrt{1+\lambda}}(\pm\zeta)$, $\zeta = \tanh\frac{\xi}{2}$, $P_3^{-2\sqrt{1+\lambda}}(\pm\zeta)$ are the Legendre functions and $c_+(\lambda)c_-(\lambda) = -\frac{1}{2}\Gamma(4+2\sqrt{1+\lambda})\Gamma(-3+2\sqrt{1+\lambda})$.

Lemma 8. *Concerning (5.1), the integral $\mathcal{G}(\lambda)$ defined in (4.31) now is*

$$\mathcal{G}(\lambda) = -108\sigma u_0\mathcal{R}(\lambda) \tag{5.9}$$

with

$$\mathcal{R}(\lambda) = \int_{-1}^{1}\int_{-1}^{\zeta} v_+(\zeta,\lambda)v_-(s,\lambda)(1-s^2)\,\mathrm{d}s\,\mathrm{d}\zeta. \tag{5.10}$$

https://doi.org/10.1017/S0956792525100132 Published online by Cambridge University Press

By Lemma 2, we denote $u_{\pm}(\chi,\lambda)$ the solutions to the following equation:

$$u_{\chi\chi} = \left(\alpha_i - d\gamma_i u_{p,0}^{d-1}(\chi) + \lambda\right) u \tag{5.11}$$

with the boundary condition $\lim_{\chi\to-\infty} u_{\pm}(\chi)e^{\mp\sqrt{\alpha_1+\lambda}\chi} = 1$. It then follows from Theorem 2 that $t_{s,+}(\lambda) = 0$ if and only if $u_+(0,\lambda) = 0$ or

$$-54\sigma u_0 \mathcal{R}(\lambda) + \frac{p_+(0,\lambda)}{u_+(0,\lambda)} = 0.$$

Theorem 6. *Let the conditions in Theorem 3 be satisfied, then*

(i) When $u_0(h) = u_0^+(h)$, if

$$\sqrt{\frac{\alpha_2+\lambda}{\alpha_2+\sqrt{\alpha_2^2+72\sigma^2 h}}}\left(1 - \frac{2}{\left(1+\frac{2}{\sqrt{\frac{\alpha_2+\lambda}{\alpha_1+\lambda}}-1}\right)e^{2\sqrt{\alpha_2+\lambda}}+1}\right) = 9\sqrt{2}\mathcal{R}(\lambda) \tag{5.12}$$

admits $\lambda \in \{\lambda \mid Re\,\lambda > 0\}$, then the pinned pulse in equation (5.1) is unstable.

(ii) When $u_0(h) = u_0^-(h)$, if

$$\sqrt{\frac{\alpha_2+\lambda}{\alpha_2-\sqrt{\alpha_2^2+72\sigma^2 h}}}\left(1 - \frac{2}{\left(1+\frac{2}{\sqrt{\frac{\alpha_2+\lambda}{\alpha_1+\lambda}}-1}\right)e^{2\sqrt{\alpha_2+\lambda}}+1}\right) = 9\sqrt{2}\mathcal{R}(\lambda) \tag{5.13}$$

admits $\lambda \in \{\lambda \mid Re\,\lambda > 0\}$, then the pinned pulse in equation (5.1) is unstable.

Proof. Now equation (5.11) turns out to be

$$u_{\chi\chi} = (f(\chi)+\lambda)u. \tag{5.14}$$

Hence,

$$u_+(\chi,\lambda) = \begin{cases} e^{\sqrt{\alpha_1+\lambda}\chi}, & \chi < -L, \\ M_1 e^{\sqrt{\alpha_2+\lambda}\chi} + N_1 e^{-\sqrt{\alpha_2+\lambda}\chi}, & -L < \chi < 0, \end{cases} \tag{5.15}$$

and

$$u_-(\chi,\lambda) = \begin{cases} e^{-\sqrt{\alpha_1+\lambda}\chi}, & \chi < -L, \\ M_2 e^{\sqrt{\alpha_2+\lambda}\chi} + N_2 e^{-\sqrt{\alpha_2+\lambda}\chi}, & -L < \chi < 0. \end{cases} \tag{5.16}$$

We choose the free parameters $M_i, N_i, i = 1,2$ such that $u_{\pm}(\chi,\lambda)$ is continuously differentiable at $\chi = -L$. Consequently,

$$\begin{pmatrix} e^{-\sqrt{\alpha_2+\lambda}L} & e^{\sqrt{\alpha_2+\lambda}L} \\ -\sqrt{\alpha_2+\lambda}\,e^{-\sqrt{\alpha_2+\lambda}L} & \sqrt{\alpha_2+\lambda}\,e^{\sqrt{\alpha_2+\lambda}L} \end{pmatrix}\begin{pmatrix} M_1 \\ N_1 \end{pmatrix} = \begin{pmatrix} e^{-\sqrt{\alpha_1+\lambda}L} \\ -\sqrt{\alpha_1+\lambda}\,e^{-\sqrt{\alpha_1+\lambda}L} \end{pmatrix}, \tag{5.17}$$

and further by the reversibility symmetry, we get

$$\begin{aligned} M_1 = N_2 &= \frac{\left(\sqrt{\alpha_1+\lambda}+\sqrt{\alpha_2+\lambda}\right)e^{\left(\sqrt{\alpha_2+\lambda}-\sqrt{\alpha_1+\lambda}\right)L}}{2\sqrt{\alpha_2+\lambda}}, \\ N_1 = M_2 &= \frac{\left(\sqrt{\alpha_2+\lambda}-\sqrt{\alpha_1+\lambda}\right)e^{-\left(\sqrt{\alpha_1+\lambda}+\sqrt{\alpha_2+\lambda}\right)L}}{2\sqrt{\alpha_2+\lambda}}. \end{aligned} \tag{5.18}$$

https://doi.org/10.1017/S0956792525100132 Published online by Cambridge University Press

This results in $u_+(0,\lambda) = M_1 + N_1 \neq 0$ and

$$\frac{p_+(0,\lambda)}{u_+(0,\lambda)} = \sqrt{\alpha_2+\lambda}\left(1 - \frac{2}{\frac{\sqrt{\alpha_2+\lambda}+\sqrt{\alpha_1+\lambda}}{\sqrt{\alpha_2+\lambda}-\sqrt{\alpha_1+\lambda}}\, e^{2\sqrt{\alpha_2+\lambda}} + 1}\right).$$

Combining (3.12) with (5.9) gives

$$\mathcal{G}(\lambda) = \begin{cases} -18\sqrt{2}\left(\alpha_2 + \sqrt{\alpha_2^2 + 72\sigma^2 h}\right)^{\frac{1}{2}} \mathcal{R}(\lambda), & u_0(h) = u_0^+(h), \\ -18\sqrt{2}\left(\alpha_2 - \sqrt{\alpha_2^2 + 72\sigma^2 h}\right)^{\frac{1}{2}} \mathcal{R}(\lambda), & u_0(h) = u_0^-(h). \end{cases} \tag{5.19}$$

Based on the results of Theorem 2, we accordingly get (5.12) and (5.13). □

Theorem 7. *Let $\varepsilon > 0$ be sufficiently small, and let $\alpha_1,\ \alpha_2 > 0,\ \gamma_1,\ L > 0,\ \gamma_2 = 0$ and $d > 1$ be fixed such that equation (5.1) admits a pinned pulse solution, then this pulse is unstable if*

$$P_\nu^\mu(z_L) + \frac{P(\lambda)}{\sqrt{\alpha_2+\lambda}} \tanh\sqrt{\alpha_2+\lambda}\, L = 0 \tag{5.20}$$

or

$$-9\sqrt{2}\mathcal{R}(\lambda) + \sqrt{\frac{\alpha_2+\lambda}{\alpha_2 \pm \sqrt{\alpha_2^2+72\sigma^2 h}}} \cdot \frac{P_\nu^\mu(z_L)\tanh\sqrt{\alpha_2+\lambda}\, L + \frac{P(\lambda)}{\sqrt{\alpha_2+\lambda}}}{P_\nu^\mu(z_L) + \frac{P(\lambda)}{\sqrt{\alpha_2+\lambda}}\tanh\sqrt{\alpha_2+\lambda}\, L} = 0, \tag{5.21}$$

possesses $\lambda \in \{\lambda \mid Re\ \lambda > 0\}$, where

$$P(\lambda) := \frac{(1-d)\sqrt{\alpha_1}}{2}\left((\nu-\mu)P_{\nu-1}^{-\mu}(z_L) + z_L \nu P_\nu^{-\mu}(z_L)\right),$$

$$z_L := \tanh\left(\frac{1}{2}(d-1)\sqrt{\alpha_1}(L + sign(p_{in})x_*)\right).$$

in which $P_\nu^\mu(z)$ and $P_\nu^\mu(-z)$ are the Legendre functions and x_* is defined by (3.25).

Proof. In the slow interval $(-\infty, -L)$, to leading order, equation (5.11) is governed by

$$u_{\chi\chi} = \left(\alpha_1 + \lambda - d\gamma_1 u_{h,-}^{d-1}(\chi)\right) u, \tag{5.22}$$

whose solution is denoted by $u_{h,-}(\chi)$,

Introducing the Hopf-cole transformation

$$z(\chi) = \tanh\left(\frac{1}{2}(d-1)\sqrt{\alpha}(\chi - \text{sign}(p_{in})x_*)\right) \tag{5.23}$$

to equation (5.22) yields the Legendre differential equation,

$$(1-z^2)u_{zz} - 2zu_z + \left(\nu(\nu+1) - \frac{\mu^2}{1-z^2}\right) u = 0, \tag{5.24}$$

where

$$\nu = \frac{d+1}{d-1}, \qquad \mu = \frac{2}{d-1}\sqrt{1+\frac{\lambda}{\alpha_1}}. \tag{5.25}$$

The solutions of (5.24) can be given in terms of the Legendre functions $P_\nu^\mu(z)$ and $P_\nu^\mu(-z)$. In light of the results in Lemma 2, we have

$$\begin{aligned} u_+(\chi) =& \Gamma(1+\mu)e^{-\Lambda_3(\lambda)x_*} P_\nu^{-\mu}(-z(\chi)) \\ =& e^{\sqrt{\alpha_1+\lambda}\chi} F\left(\nu+1, -\nu, 1+\mu, \frac{1}{2} + \frac{1}{2}z(\chi)\right) \end{aligned} \tag{5.26}$$

https://doi.org/10.1017/S0956792525100132 Published online by Cambridge University Press

satisfying $u_+(\chi)\to 0$ as $\chi\to-\infty$. To further simplify the notation, let us introduce

$$\begin{aligned} u(-L,\lambda) &:= \lim_{\chi\uparrow -L} u_+(\chi) = \Gamma(1+\mu)e^{-\Lambda_3(\lambda)x_*}P_\nu^\mu\big(z_L\big),\\ p(-L,\lambda) &:= \lim_{\chi\uparrow -L} p_+(\chi) = \frac{(1-d)\sqrt{\alpha_1}}{2}\Gamma(1+\mu)e^{-\Lambda_3(\lambda)x_*}\left[(\nu-\mu)P_{\nu-1}^{-\mu}\big(z_L\big)+z_L\nu P_\nu^{-\mu}\big(z_L\big)\right], \end{aligned} \tag{5.27}$$

in which

$$z_L := \tanh\left(\frac{1}{2}(d-1)\sqrt{\alpha}(L+\operatorname{sign}(p_{in})x_*)\right).$$

Moreover, by following Lemma 6, we have

$$u_+(\chi,\lambda) = \begin{cases} \Gamma(1+\mu)e^{-\Lambda_3(\lambda)x_*}P_\nu^{-\mu}\big(-z(\chi)\big), & \chi<-L,\\ M_3e^{\sqrt{\alpha_2+\lambda}\,\chi}+N_3e^{-\sqrt{\alpha_2+\lambda}\,\chi}, & -L<\chi<0, \end{cases} \tag{5.28}$$

where

$$\begin{aligned} M_3 &= \frac{u(-L,\lambda)\sqrt{\alpha_2+\lambda}+p(-L,\lambda)}{2\sqrt{\alpha_2+\lambda}}\,\mathrm{e}^{\sqrt{\alpha_2+\lambda}\,L},\\ N_3 &= \frac{u(-L,\lambda)\sqrt{\alpha_2+\lambda}-p(-L,\lambda)}{2\sqrt{\alpha_2+\lambda}}\,\mathrm{e}^{-\sqrt{\alpha_2+\lambda}\,L}. \end{aligned} \tag{5.29}$$

As a consequence,

$$\begin{aligned} u_+(0,\lambda) &= u(-L,\lambda)\cosh\sqrt{\alpha_2+\lambda}\,L+\frac{p(-L,\lambda)}{\sqrt{\alpha_2+\lambda}}\sinh\sqrt{\alpha_2+\lambda}\,L,\\ p_+(0,\lambda) &= u(-L,\lambda)\sqrt{\alpha_2+\lambda}\sinh\sqrt{\alpha_2+\lambda}\,L+p(-L,\lambda)\cosh\sqrt{\alpha_2+\lambda}\,L. \end{aligned} \tag{5.30}$$

This means that $u_+(0,\lambda)p_-(0,\lambda)-u_-(0,\lambda)p_+(0,\lambda)=2\sqrt{\alpha_2+\lambda}(N_3^2-M_3^2)\neq 0$ and

$$\frac{p_+(0,\lambda)}{u_+(0,\lambda)} = \frac{\sqrt{\alpha_2+\lambda}\tanh\sqrt{\alpha_2+\lambda}\,L+\frac{p(-L,\lambda)}{u(-L,\lambda)}}{1+\frac{p(-L,\lambda)}{u(-L,\lambda)\sqrt{\alpha_2+\lambda}}\tanh\sqrt{\alpha_2+\lambda}\,L}. \tag{5.31}$$

Thus, (5.20) and (5.21) hold. □

Define two functions $\mathrm{B}_\pm(\chi)$ and their derivatives $\mathrm{B}'_\pm(\chi)$, respectively, by

$$\mathrm{B}_\pm(\chi) = e^{\pm\sqrt{\alpha_2+\lambda}\chi}F\left(\nu+1,-\nu,1+\mu_2,\frac{1}{2}\pm\frac{1}{2}y(\chi)\right),\qquad \mathrm{B}'_\pm(\chi)=\frac{\mathrm{d}}{\mathrm{d}\chi}\mathcal{B}_\pm(\chi). \tag{5.32}$$

Theorem 8. *Let the conditions in Theorem 4 be fulfilled. If the length of the heterogeneity L satisfies $h(L)=\mathcal{O}(\varepsilon)$, then the pinned pulse solution of equation (5.1) is unstable if $\lambda\in\{\lambda \mid Re\ \lambda>0\}$,*

$$u(-L,\lambda)B_2(\lambda)+p(-L,\lambda)B_1(\lambda)=0 \tag{5.33}$$

or

$$\frac{u(-L,\lambda)B_4(\lambda)+p(-L,\lambda)B_3(\lambda)}{u(-L,\lambda)B_2(\lambda)+p(-L,\lambda)B_1(\lambda)} = 18\sqrt{\alpha_2}y_0\mathcal{R}(\lambda) \tag{5.34}$$

https://doi.org/10.1017/S0956792525100132 Published online by Cambridge University Press

admits a root λ *with positive real part, where* $u(-L,\lambda)$ *and* $p(-L,\lambda)$ *are defined in equation (5.27), and* $y_0 = \tanh\left(\frac{(d-1)\sqrt{\alpha_2}}{2} y_*\right)$. *Furthermore, the functions* $B_1(\lambda)$, $i = 1, 2, 3, 4$, *are given by*

$$\begin{aligned} B_1(\lambda) &= B_+(-L)B_-(0) - B_-(-L)B_+(0), \\ B_2(\lambda) &= B'_-(-L)B_+(0) - B'_+(-L)B_-(0), \\ B_3(\lambda) &= B_+(-L)B'_-(0) - B_-(-L)B'_+(0), \\ B_4(\lambda) &= B'_-(-L)B'_+(0) - B'_+(-L)B'_-(0). \end{aligned}$$

Proof. First, let us consider the simple case, namely, $h(L) = 0$. In this case, equation (5.11) can be written as

$$u_{\chi\chi} = \begin{cases} \left(\alpha_1 + \lambda - d\gamma_1 u_{h,-}^{d-1}(\chi)\right) u, & \chi \in (-\infty, -L), \\ \left(\alpha_2 + \lambda - d\gamma_2 u_{i,-}^{d-1}(\chi, 0)\right) u, & \chi \in (-L, 0), \end{cases} \tag{5.35}$$

where the solutions $u_{i,-}(\chi, 0)$ and $u_{h,-}(\chi)$ are defined in equation (3.25) and (3.27), respectively. According to the result of Lemma 7, the solution $u_+(\xi, \lambda)$ is given by

$$u_+(\xi,\lambda) = \begin{cases} \Gamma(1+\mu) e^{-\Lambda_3(\lambda)x_*} P_\nu^{-\mu}\left(-z(\chi)\right), & \chi < -L, \\ M_4 e^{\sqrt{\alpha_2+\lambda}\chi} F\left(\nu+1, -\nu; 1+\mu_2, \frac{1}{2} + \frac{1}{2} y(\chi)\right) & \\ \quad + N_4 e^{-\sqrt{\alpha_2+\lambda}\chi} F\left(\nu+1, -\nu, 1+\mu_2, \frac{1}{2} - \frac{1}{2} y(\chi)\right), & -L < \chi < 0. \end{cases} \tag{5.36}$$

where

$$\mu_2 = \frac{2}{d-1}\sqrt{1 + \frac{\lambda}{\alpha_2}}, \qquad y(\chi) = \tanh\left(\frac{(d-1)\sqrt{\alpha_2}}{2}(\chi - y_*)\right), \tag{5.37}$$

and

$$\begin{aligned} M_4 &= \frac{u(-L,\lambda)\mathrm{B}'_-(-L) - p(-L,\lambda)\mathrm{B}_-(-L)}{\mathrm{B}_+(-L)\mathrm{B}'_-(-L) - \mathrm{B}_-(-L)\mathrm{B}'_+(-L)}, \\ N_4 &= \frac{\mathrm{B}_+(-L)p(-L,\lambda) - \mathrm{B}'_+(-L)u(-L,\lambda)}{\mathrm{B}_+(-L)\mathrm{B}'_-(-L) - \mathrm{B}_-(-L)\mathrm{B}'_+(-L)} \end{aligned} \tag{5.38}$$

with $u(-L,\lambda)$ and $p(-L,\lambda)$ are given by (5.27). Note that the expression for $u_+(\chi,\lambda)$ in equation (5.36) is valid only when $\lambda \neq \lambda_j$, for $j = 0, 1, \ldots, J$, where $J < \nu \leq J+1$ and $\lambda_j = \frac{1}{4}\left[(d+1) - j(d-1)\right]^2 - 1$. This restriction is generated since, when $\lambda = \lambda_j$, the pair of functions $\{P_\nu^{\mu_2}(z), P_\nu^{\mu_2}(-z)\}$ is insufficient to span the solution space of equation (5.35). Thus, we have

$$\begin{aligned} u_+(0,\lambda) =& u(-L,\lambda)\frac{\mathrm{B}'_-(-L)\mathrm{B}_+(0) - \mathrm{B}'_+(-L)\mathrm{B}_-(0)}{\mathrm{B}_+(-L)\mathrm{B}'_-(-L) - \mathrm{B}_-(-L)\mathrm{B}'_+(-L)} \\ &+ p(-L,\lambda)\frac{\mathrm{B}_+(-L)\mathrm{B}_-(0) - \mathrm{B}_-(-L)\mathrm{B}_+(0)}{\mathrm{B}_+(-L)\mathrm{B}'_-(-L) - \mathrm{B}_-(-L)\mathrm{B}'_+(-L)}, \end{aligned} \tag{5.39}$$

and

$$\begin{aligned} p_+(0,\lambda) =& u(-L,\lambda)\frac{\mathrm{B}'_-(-L)\mathrm{B}'_+(0) - \mathrm{B}'_+(-L)\mathrm{B}'_-(0)}{\mathrm{B}_+(-L)\mathrm{B}'_-(-L) - \mathrm{B}_-(-L)\mathrm{B}'_+(-L)} \\ &+ p(-L,\lambda)\frac{\mathrm{B}_+(-L)\mathrm{B}'_-(0) - \mathrm{B}_-(-L)\mathrm{B}'_+(0)}{\mathrm{B}_+(-L)\mathrm{B}'_-(-L) - \mathrm{B}_-(-L)\mathrm{B}'_+(-L)}. \end{aligned} \tag{5.40}$$

https://doi.org/10.1017/S0956792525100132 Published online by Cambridge University Press

It follows that

$$\frac{p_+(0,\lambda)}{u_+(0,\lambda)} = \frac{\mathrm{B}'_-(-L)\mathrm{B}'_+(0) - \mathrm{B}'_+(-L)\mathrm{B}'_-(0) + \frac{p(-L,\lambda)}{u(-L,\lambda)}\left(\mathrm{B}_+(-L)\mathrm{B}'_-(0) - \mathrm{B}_-(-L)\mathrm{B}'_+(0)\right)}{\mathrm{B}'_-(-L)\mathrm{B}_+(0) - \mathrm{B}'_+(-L)\mathrm{B}_-(0) + \frac{p(-L,\lambda)}{u(-L,\lambda)}\left(\mathrm{B}_+(-L)\mathrm{B}_-(0) - \mathrm{B}_-(-L)\mathrm{B}_+(0)\right)} \tag{5.41}$$

We next consider the general case, that is, $h(L) = \mathcal{O}(\varepsilon)$. We can further derive the solution to equation (5.11) by using perturbation analysis. First, recall that the Hamiltonian value $h(L) = 0$ corresponds to the homoclinic orbit in the 2nd system. Thus, for $h(L) = \mathcal{O}(\varepsilon)$, the orbit is located near this homoclinic orbit. Moreover, when $\varepsilon > 0$ is sufficiently small, the distance between the two orbits becomes very small. Specifically, when $h(L) = \mathcal{O}(\varepsilon)$, equation (5.11) can be regarded as a small perturbation of equation (5.35). It is easy to verify that equation (5.35) exhibits exponential dichotomy on the regions $\mathbb{R}_\pm$. By the principle of exponential dichotomy and its robustness, the stable and unstable spaces of equation (5.11) are $\mathcal{O}(\varepsilon)$-close to those of equation (5.35). Thus, equations (5.39) and (5.40) remain valid when $h(L) = \mathcal{O}(\varepsilon)$.

Let

$$y_0 = -y(0) = \tanh\left(\frac{(d-1)\sqrt{\alpha_2}}{2} y_*\right).$$

We next use y_0 to express u_0. Using the fact that the jump point (u_0, p_0) is the intersection of the Take-off curve and the orbit defined by $H_s(u,p) = 0$, we obtain the following relations:

$$u_{0,\chi}^2 = \alpha_2 u_0^2 - \frac{\gamma_2}{d+1} u_0^{d+1},$$

$$u_{0,\chi} = 3\sigma u_0^2.$$

Combining (3.27) and (5.37) gives $y^2(\chi) = \frac{1}{\alpha_2}\frac{u_\chi^2}{u^2}$. Therefore, we have the following relationship:

$$\alpha_2(1 - y_0^2) = \frac{2\gamma_2}{d+1} u_0^{d-1} = (\alpha_2 - 9\sigma^2 u_0^2),$$

which gives

$$u_0 = \frac{\sqrt{\alpha_2} y_0}{3\sigma}. \tag{5.42}$$

By combining the conclusions from Theorem 2 and Lemma 8, we obtain equations (5.33) and (5.34). Based on (5.33) or (5.34), we can identify the signs of the eigenvalues λ numerically under certain parameter values. In this manner, we can judge whether the pinned pulses is stable or unstable under the present parameter condition. □

Remark 15. If the non-autonomous GM equation reduces to the autonomous one, that is, $f(\chi) \equiv \alpha_1$ and $g(\chi) \equiv \beta_1$ in equation (5.1), which had been studied in Veerman and Doelman [37], in this case, we have $L = 0$. Hence, (5.39) and (5.40), respectively, reduce to

$$\begin{aligned} u_+(0,\lambda) =& \Gamma(1+\mu) e^{-\Lambda_3(\lambda)x_*} P_\nu^{-\mu}(z_*), \\ p_+(0,\lambda) =& \frac{(1-d)\sqrt{\alpha_1}}{2} \Gamma(1+\mu) e^{-\Lambda_3(\lambda)x_*} \left((\nu-\mu) P_{\nu-1}^{-\mu}(z_*) + z_* \nu P_\nu^{-\mu}(z_*)\right) \end{aligned} \tag{5.43}$$

with $z_* = \mathrm{sign}(\sigma)\tanh\left(\frac{1}{2}(d-1)\sqrt{\alpha_1}\, x_*\right)$. That is, the instability criterion (5.33) and (5.34), respectively, reduce to

$$P_\nu^{-\mu}(z_*) = 0$$

or

$$\frac{1}{\nu - 1}\left(\nu - (\nu-\mu)\frac{P_{\nu-1}^{-\mu}(z_*)}{z_* P_\nu^{-\mu}(z_*)}\right) = 18\mathcal{R}(\lambda),$$

which are identical with which in [37, Corollary 4.1] for the autonomous GM equation with a slow nonlinearity.

https://doi.org/10.1017/S0956792525100132 Published online by Cambridge University Press

Financial support. The research is supported by the National Science Foundation (NSF) of China (No. 12271096), the NSF of Fujian Province (No. 2022J02028) and the Young Top Talent of Fu-jian Young Eagle Program.

Competing interests. The authors declare that they have no known competing financial interests or personal relationships that could have appeared to influence the work reported in this paper.

References

[1] Alexander, J., Gardner, R. A. & Jones, C. K. R. T. (1990) A topological invariant arising in the stability analysis of travelling waves. *J. Reine Angew. Math.* **410**, 167–212.
[2] Avitabile, D., Brena, V. F. & Ward, M. J. (2018) Spot dynamics in a reaction–diffusion model of plant root hair initiation. *SIAM J. Appl. Math.* **78**(1), 291–319.
[3] Bastiaansen, R., Chirilus-Bruckner, M. & Doelman, A. (2020) Pulse solutions for an extended Klausmeier model with spatially varying coefficients. *SIAM J. Appl. Dyn. Syst.* **19**(1), 1–57.
[4] Benson, D. L., Maini, P. K. & Sherratt, J. A. (1993) Spatial asymmetry in chemical pattern formation: A turing model for biological patterning. *Bull. Math. Biol.* **55**(2), 365–384.
[5] Byrnes, E., Carter, P., Doelman, A. & Liu, L. (2023) Large amplitude radially symmetric spots and gaps in a dryland ecosystem model. *J. Nonlinear Sci.* **33**(6), 107.
[6] Chen, W. & Ward, M. J. (2009) Oscillatory instabilities and dynamics of multi-spike patterns for the one-dimensional Gray–Scott model. *Eur. J. Appl. Math.* **20**(2), 187–214.
[7] Chen, Y., Li, J., Shen, J. & Zhang, Q. (2024) Pattern formations in nonlinear reaction–diffusion systems with strong localized impurities. *J. Differ. Equ.* **402**, 250–289.
[8] Chen, Y. & Shen, J. (2025) Pulse solutions in Gierer–Meinhardt equation with slowly degenerate nonlinearity. *Physica D*, **481**, 134738.
[9] Coppel, W. A. (1965). *Stability and Asymptotic Behavior of Differential Equations*, Boston, D.C. Heath and Co
[10] de Rijk, B., Doelman, A. & Rademacher, J. (2016) Spectra and stability of spatially periodic pulse patterns: Evans function factorization via Riccati transformation. *SIAM J. Math. Anal.* **48**(1), 61–121.
[11] Derks, G., Doelman, A., Knight, C. J. & Susanto, H. (2012) Pinned fluxons in a Josephson junction with a finite-length inhomogeneity. *European J. Appl. Math.* **23**(2), 201–244.
[12] Doelman, A., Gardner, R. A. & Kaper, T. J. (2001) Large stable pulse solutions in reaction–diffusion equations. *Indiana Univ. Math. J.* **50**, 443–507.
[13] Doelman, A., Gardner, R. A. & Kaper, T. J. (2002) *A Stability Index Analysis of 1-D Patterns of the Gray–Scott Model*, American Mathematical Society.
[14] Doelman, A., Iron, D. & Nishiura, Y. (2004) Destabilization of fronts in a class of bistable systems. *SIAM J. Math. Anal.* **35**(6), 1420–1450.
[15] Doelman, A., Van Heijster, P. & Shen, J. (2018) Pulse dynamics in reaction–diffusion equations with strong spatially localized impurities. *Philo. Trans. Royal Soc. A* **376**(2117), 20170183.
[16] Doelman, A. & Veerman, F. (2015) An explicit theory for pulses in two component, singularly perturbed, reaction–diffusion equations. *J. Dyn. Differ. Equ.* **27**, 555–595.
[17] Fenichel, N. (1979) Geometric singular perturbation theory for ordinary differential equations. *J. Differ. Equ.* **31**(1), 53–98.
[18] Gardner, R. A. & Jones, C. K. R. T. (1991) Stability of travelling wave solutions of diffusive predator–prey systems. *Amer. Math. Soc.* **327**(2), 465–524.
[19] Iron, D., Ward, M. J. & Wei, J. (2001) The stability of spike solutions to the one-dimensional Gierer–Meinhardt model. *Physica D* **150**(1-2), 25–62.
[20] Kapitula, T. & Promislow, K. (2013). *Spectral and Dynamical Stability of Nonlinear Waves*, vol. New York, Springer, Vol. **457**.
[21] Knight, C. J., Derks, G., Doelman, A. & Susanto, H. (2013) Stability of stationary fronts in a non-linear wave equation with spatial inhomogeneity. *J. Differ. Equ.* **254**(2), 408–468.
[22] Kong, F., Ward, M. J. & Wei, J. (2024) Existence, stability and slow dynamics of spikes in a 1D minimal Keller–Segel model with logistic growth. *J. Nonlinear Sci.* **34**(3), 51.
[23] Li, J. & Yu, Q. (2023) Simple and multiple traveling waves in a reaction–diffusion-mechanics model. *J. Differ. Equ.* **377**, 578–621.
[24] Meinhardt, H. & Gierer, A. (2000) Pattern formation by local self-activation and lateral inhibition. *BioEssays* **22**(8), 753–760.
[25] Morimoto, K. (2009) Construction of multi-peak solutions to the Gierer–Meinhardt system with saturation and source term. *Nonlinear Anal.* **71**(7-8), 2532–2557.
[26] Muratov, C. & Osipov, V. (2001) Spike autosolitons and pattern formation scenarios in the two-dimensional Gray–Scott model. *Eur. Phys. J. B* **22**, 213–221.
[27] Page, K., Maini, P. K. & Monk, N. A. (2003) Pattern formation in spatially heterogeneous turing reaction–diffusion models. *Physica D* **181**(1-2), 80–101.
[28] Palmer, K. J. (1986) Transversal heteroclinic points and Cherry's example of a nonintegrable Hamiltonian system. *J. Differ. Equ.* **65**(3), 321–360.

[29] Qiao, Q. & Zhang, X. (2023) Traveling waves and their spectral stability in Keller–Segel system with large cell diffusion. *J. Differ. Equ.* **344**, 807–845.
[30] Robinson, C. (1983) Sustained resonance for a nonlinear system with slowly varying coefficients. *SIAM J. Math.* **14**(5), 847–860.
[31] Sewalt, L. & Doelman, A. (2017) Spatially periodic multipulse patterns in a generalized Klausmeier–Gray–Scott model. *SIAM J. Appl. Dyn. Syst.* **16**(2), 1113–1163.
[32] Siero, E., Doelman, A., Eppinga, M., Rademacher, J. D., Rietkerk, M. & Siteur, K. (2015) Striped pattern selection by advective reaction–diffusion systems: Resilience of banded vegetation on slopes. *Chaos* **25**(3), 036411.
[33] Sun, W., Ward, M. J. & Russell, R. (2005) The slow dynamics of two-spike solutions for the Gray–Scott and Gierer–Meinhardt systems: Competition and oscillatory instabilities. *SIAM J. Appl. Dyn. Syst.* **4**(4), 904–953.
[34] Turing, A. M. (1952) The chemical basis of morphogenesis. *Trans. Roy. Soc. Lond. Ser. B* **237**, 37–72.
[35] Tzou, J., Xie, S., Kolokolnikov, T. & Ward, M. J. (2017) The stability and slow dynamics of localized spot patterns for the 3-D Schnakenberg reaction–diffusion model. *SIAM J. Appl. Dyn. Syst.* **16**(1), 294–336.
[36] Van Heijster, P., Doelman, A., Kaper, T. J., Nishiura, Y. & Ueda, K.-I. (2010) Pinned fronts in heterogeneous media of jump type. *Nonlinearity* **24**(1), 127.
[37] Veerman, F. & Doelman, A. (2013) Pulses in a Gierer–Meinhardt equation with a slow nonlinearity. *SIAM J. Appl. Dyn. Syst.* **12**(1), 28–60.
[38] Wei, J. (1999) Existence, stability and metastability of point condensation patterns generated by the Gray–Scott system. *Nonlinearity* **12**(3), 593.
[39] Wei, J. & Winter, M. (2009) Spikes for the Gierer–Meinhardt system with discontinuous diffusion coefficients. *J. Nonlinear Sci.* **19**, 301–339.
[40] Wei, J., Winter, M. & Yang, W. (2017) Stable spike clusters for the precursor Gierer–Meinhardt system in $\mathbb{R}^2$. *Calc. Var. Part. Differ. Equ.* **56**, 1–40.

Cite this article: Chen Y. and Shen J. A geometric approach to pinned pulses in a class of non-autonomous reaction–diffusion equations. *European Journal of Applied Mathematics*, https://doi.org/10.1017/S0956792525100132